

# Topology Control for Directed Data Links between Airborne Platforms

## Directed Air Data Link: WP3 report

Dragos Ilie, Håkan Grahm, Lars Lundberg, Alexander Westerhagen



**Vinnova NFFP7**

**Directed data link**

**Blekinge Institute of Technology (BTH)**

371 79 Karlskrona, Sweden

# Summary

---

Contemporary airborne radio networks are usually implemented using omnidirectional antennas. Unfortunately, such networks suffer from disadvantages such as easy detection by hostile aircraft and potential information leakage. In addition, tactical links used for military communication rely on NATO-specific standards such as Link 16, which are becoming outdated.

To this end we are investigating the feasibility of replacing omnidirectional communication with directed communication, which will address the disadvantages mentioned above. In addition, we define a communication architecture based on the conventional Ethernet and TCP/IP protocol stack, which will ease management and interoperability with existing Internet-based system

In this report, we briefly review the TCP/IP stack and the services offered at each layer of the stack. Furthermore, we review existing literature involving mobile ad hoc network (MANET) protocols used for airborne networks along with various performance studies in the same area. Finally, we propose a novel MANET routing protocol based on directional antennas and situation awareness data that utilizes adaptive multihop routing to avoid sending information in directions where hostile nodes are present.

Our protocol is implemented in the OMNEST simulator and evaluated using two realistic flight scenarios involving 8 and 24 aircraft, respectively. The results show that our protocol has significantly fewer leaked packets than comparative protocols, but at a slightly higher cost in terms of longer packet lifetime.



# Contents

---

<b>Summary</b>	<b>i</b>
<b>Contents</b>	<b>iii</b>
<b>List of Figures</b>	<b>v</b>
<b>1 Introduction</b>	<b>1</b>
<b>2 TCP/IP stack and routing</b>	<b>3</b>
2.1 TCP/IP stack overview . . . . .	3
2.2 Services provided by the physical layer . . . . .	3
2.3 Services provided by the link layer . . . . .	4
2.4 Services provided by the network layer (IPv4) . . . . .	5
2.5 Routing algorithms and protocols . . . . .	6
<b>3 Conceptual architecture</b>	<b>9</b>
3.1 Physical layer . . . . .	10
3.2 Link layer – Ethernet II . . . . .	11
3.3 Network Layer – IPv4 . . . . .	11
3.4 Multicast and broadcast . . . . .	12
<b>4 Use cases</b>	<b>13</b>
4.1 Situation awareness data . . . . .	13
4.2 Example use cases . . . . .	14
<b>5 HDARP</b>	<b>17</b>
5.1 Forbidden Sector Detection . . . . .	19
<b>6 Simulation framework</b>	<b>25</b>
6.1 InterceptApp . . . . .	27
6.2 UdpBasicApp . . . . .	28
6.3 Simulation Scenarios . . . . .	28
6.4 Simulation Settings . . . . .	30
6.5 Simulation results . . . . .	32
6.6 Analysis and Discussion . . . . .	37
<b>7 Related work</b>	<b>39</b>

7.1	Reducing transmission detection . . . . .	39
7.2	Architecture, Design . . . . .	40
7.3	Specifications, on-track, or well-known . . . . .	41
7.4	Surveys . . . . .	42
<b>8</b>	<b>Conclusion and Future Work</b>	<b>45</b>
	<b>Bibliography</b>	<b>47</b>

# List of Figures

---

3.1	Conceptual architecture . . . . .	10
3.2	Network architecture . . . . .	11
4.1	Two friendly aircraft communicating with each other . . . . .	15
4.2	Three friendly aircraft communicating with each other, using both single-hop routing and multi-hop routing . . . . .	16
4.3	Three friendly aircraft communicating with each other, but with an adversary nearby forcing multi-hop routing to be used . . . . .	16
5.1	Forbidden sector detection. To the left: 3D view of detector operation. To the right: cross-section of 3D radiation pattern with detector. Ratio between size of main lobe and size of sidelobes is decreased on purpose in order for the sidelobes to be visible in the figure. . . . .	21
6.1	Simulation scenarios. Upper: Scenario 1. Lower: Scenario 2. Maps data: Google ©2023. . . . .	29
6.2	Average number of leaked packets when using directional antennas (99% confidence interval), for Scenario 1 ( <b>upper</b> ) and Scenario 2 ( <b>lower</b> ). . . . .	34
6.3	Average packet life time in seconds (99% confidence interval) when using omnidirectional antennas for all protocols except HDARP (HDARP uses directional antennas) for Scenario 1 ( <b>upper</b> ) and Scenario 2 ( <b>lower</b> ). . . . .	35
6.4	Average packet delivery ratio in percent (99% confidence interval) when using omnidirectional antennas for all protocols except HDARP (HDARP uses directional antennas) for Scenario 1 ( <b>upper</b> ) and Scenario 2 ( <b>lower</b> ). . . . .	36
6.5	Average number of packets sent over the radio interface (99% confidence interval) when using omnidirectional antennas for all protocols except HDARP (HDARP uses directional antennas) for Scenario 1 ( <b>upper</b> ) and Scenario 2 ( <b>lower</b> ). . . . .	37





# CHAPTER 1

## Introduction

---

Recent developments within the aerospace industry indicate that an increasing proportion of aerospace products will consist of cooperative platforms, in particular between autonomous platforms such as aircraft, ships, missiles, drones and decoys.

Conventional radio communication between airborne platforms is usually implemented using antennas that radiate signal power omnidirectionally. A disadvantage associated with this approach is that the transmission power is not concentrated towards the receiver. This limits the communication range between nodes in a multihop scenario, increases power requirements, but more importantly, it simplifies detection/positioning by an adversary from arbitrary location.

Nowadays, the adversaries that can control and deny access to the electromagnetic (EM) spectrum will have a substantial advantage in a potential conflict. Thus, EM superiority may be considered as a vital military ability, which generates an ever increasing stream of powerful interferers and capable electronic warfare (EW) devices.

This situation motivates a departure from omnidirectional transmission towards directed communication in order obtain communication solutions with low probability of intercept/detection (LPI/LPD). Furthermore, if the receiver antennas are of digital multi-channel type further advantages can be achieved, such as simultaneous reception at the same frequency, asynchronous or reactive reception and adaptive noise suppression [1].

In addition, the use of mobile ad-hoc networks (MANETs) would enable multihop communication bringing additional benefits such as increased range of communication and robustness to network dynamics through the use of multiple paths between communicating nodes. However, in military heterogeneous environments involving airborne nodes, terrestrial units, as well as nodes at sea and in space, multihop routing suffers from several issues such as: poor interoperability, heterogeneous software interfaces, non-standard link information reported by the involved radios, significant manual setup and configuration [2].

This project attempts to address these shortcomings by:

- Employing directed communication through beamforming with active electronically scanned array (AESA) antennas.
- Replacing the proprietary communication stack with the widely adopted TCP/IP stack, with minor adaptations for directed communication.
- Adapting existing MANET routing algorithms for multi-hop communication.

It is crucial that the pilots of military aircraft have access to updated information about the location of friendly and hostile aircraft. This kind of information is provided through so-called *situation awareness (SA) data*. SA data contain, among other things, the location, direction and speed of friendly and hostile aircraft in an area.

We define the concept of the *leaked packet*. A leaked packet is a unit of data transmitted with a radio carrier wave that can be detected by an adversary aircraft. A packet is considered to be leaked even if the received radio signal to noise ratio (SNR) is so low that the adversary cannot receive and decode the data<sup>1</sup>.

However, it is enough that the adversary can discern the radio signal carrying the packet from electromagnetic noise. Adversaries can use this information to track the position of the transmitting aircraft.

In this report, we present a routing protocol for airborne tactical networks. The protocol is called the *Hostile-Direction Aware Routing Protocol (HDARP)*. The protocol requires nodes to be equipped with directional antennas and makes use of SA data to route packets from the sender to the receiver (including multi-hop routing when needed), while at the same time avoiding adversary detection/positioning by eliminating leaked packets. HDARP is intended to be used together with the widely adopted TCP/IP stack, with minor adaptations for directed communication. HDARP is protected by patent application SE 2200136-6, and is also published in *Future Internet* [3]<sup>2</sup>.

---

<sup>1</sup>Data on tactical links is typically encrypted, which makes decoding infeasible.

<sup>2</sup>Published under Creative Commons license CC BY 4.0 <https://creativecommons.org/licenses/by/4.0/>

# CHAPTER 2

## TCP/IP stack and routing

---

### 2.1 TCP/IP stack overview

Formally, the TCP/IP architecture model consists of four layers: application layer, transport layer (TCP/UDP), network layer (IP) and link layer [4]. However, there is always an implicit assumption of a fifth layer, the physical layer, which carries out the actual transmission and reception of information to/from the communication medium.

In our case, the physical layer is implemented through the AESA antennas and the controls associated with them. Details about the physical layer are outside the scope of this document, with the exception of services exposed towards the link layer. The transport layer will consist of the TCP and UDP protocols that will be used without any modifications to the original specification. The application layer consists of all the required applications and services installed on the platform. They are not within the scope of this work.

### 2.2 Services provided by the physical layer

The physical layer is responsible for the transmission and reception of digital bitstreams across the communication medium (i.e., radio). This includes any signal processing required for encoding, modulation, error-coding and such.

The physical layer offers four services:

- Transmission of a link layer frame
- Reception of a complete link layer frame
- Error notification
- Access to radio channel statistics per destination node: bitrate, bit error rate (BER), link quality metric etc. (NOTE: this maybe offered separately through situation awareness (SA) data).

The AESA resources are typically shared with electronic warfare (EW) systems aboard the military aircraft. The EW systems have always higher priority to AESA resources and therefore communication (COM) systems may lose temporarily access to

those resources. Auxiliary functions in the COM stack (such as packet scheduling, time-stamping, feedback to application layer etc.) must be designed to continue to operate in this impaired state (i.e., graceful degradation).

## 2.3 Services provided by the link layer

The link layer is responsible for the transmission and reception of link frames between directly reachable nodes. A node is directly reachable from another node when

1. Its physical layer is able to receive bitstreams from the physical layer of its peer with a high probability
2. None of the nodes is located in a forbidden sector/direction where communication can knowingly be intercepted by an adversary (as indicated by SA)
3. The peer node is allowed to receive transmissions from the sending node (as indicated by SA)

Implicitly, the link layer provides the abstraction of one unidirectional one-hop link towards each of the peering nodes. The local end of the a link corresponds to the typical network interface controller (NIC) found on commercial-off-the-shelf (COTS) computers. A NIC is also frequently referred to as an interface. Each interface needs to be assigned a unique media access control (MAC) address. The MAC address of the remote end of the link is revealed when a link layer frame is received from the peering node.

The link layer can also operate in additional modes described below: unicast mode, promiscuous mode, multicast mode, broadcast mode. The availability of the modes is configurable.

The AESA array is capable of receiving simultaneous communication from multiple senders. In unicast mode, the link layer propagates up the stack the payload from a received frame, only if the destination MAC address found in the link layer header matches the MAC address assigned to the receiving interface.

However, if the interface is set to promiscuous mode all received frames are propagated up the stack, irrespective of the destination link address. This can be useful for diagnosis purposes, but can also be used for example to support intrusion prevention systems (IPSs) that require access to raw traffic.

A part of the MAC address space can be reserved for so called group addresses that are used in multicast communication (one-to-many). In this case, the receiver configures the link layer to listen to specific group addresses in addition to the configured MAC addresses [5]. The group addresses can be configured per node or per link. In addition, the receiver may specify eligible senders for the group address. The sender configures the stack to use a specific group address as destination address in a link layer frame and all link layers listening on the specific group propagate the received packet up the stack. Note that link layer group addresses are mapped to network layer group addresses. The

network layer will not process the payload from a received multicast frame unless such mapping was correctly configured.

A MAC address consisting only of 1s is reserved as broadcast address. Frames using the broadcast address as destination address are always propagated up the stack by the receiver.

The link layer offers the following services:

- Transmission of a network (IPv4 or ARP) layer packet. Additional protocols on top of the link layer can be supported if necessary.
- Reception of a valid network (IPv4 or ARP) layer packet. Additional protocols on top of the link layer can be supported if necessary.
- Link status (up/down) for each directly reachable peer.
- Error notification.

The link layer is usually implemented as part of the operating system (OS), that exposes the link abstraction to user-space in the form of a network device. Thus, OS primitives can be used to specify synchronous or asynchronous operation.

## 2.4 Services provided by the network layer (IPv4)

The network layer is responsible for the transmission and reception of data units from upper layers (TCP or UDP). In addition, this layer implements a MANET routing protocol to enable communication with nodes that are not directly connected. Directly connected nodes use the routing protocol to exchange information about remote destinations for which they can act as intermediate nodes. A node is eligible to be used as intermediate node if it has two or more established links (cf. Section 2.3). This is referred to as *interior MANET* routing [6].

Furthermore, the network layer provides a hierarchical addressing scheme enabling interfaces to be grouped into networks and subnetworks (subnets). A typical network layer address is of the form <network>.<subnet>.<interface>. Such an address is assigned to each of the link layer interfaces, in addition to the existing MAC address. The MAC address is necessary for transport within a subnet, whereas the network layer address is used for transport between subnets and networks.

Consequently, there can be multiple airborne MANETs that need to communicate with each other and with mobile or fixed infrastructure on the ground or on water. Therefore some of the nodes must have the capabilities to work as access routers between separate networks, quite likely having to run additional routing protocols concurrently with the MANET protocol. This is referred to as *exterior MANET* routing [6].

The different subnets may serve different organizational purposes, may have different ownership and most likely will use different security classification levels. Therefore, packet-filtering firewalls and specific sets of cryptographic primitives will be required to implement policies for information flows. However, this is outside the scope of this report.

Furthermore, the network layer reserves part of the network address spaces to network group addresses. These are mapped to link layer group addresses, as mentioned in Section 2.3 and are used for multicast communication. To enable multicast communication across subnets a group management protocol is necessary, such as the Internet Group Management Protocol (IGMP) [7].

The network layer offers the following services:

- Transmission of a transport layer data unit.
- Reception of a valid transport layer data unit.
- Multi-hop path establishment via MANET routing protocol.
- Packet-forwarding to different networks and subnets.
- Error notification.

## 2.5 Routing algorithms and protocols

Every node in a communication network maintains a *link state* for each of its links. The link state consists of configured operational parameters (e.g., MAC and network address) and a set of quality of service (QoS) metrics (e.g., bitrate, maximum transmission unit (MTU), round-trip time (RTT) and perhaps a cost value).

Nodes use a process called *routing* to find paths (routes) between themselves and other nodes in the network. The routing process consists of a routing protocol and a routing algorithm. The protocol allows nodes to exchange topology information, which allows them to gradually discover other nodes in the network. The discovered nodes are stored in a routing table. The routing algorithm processes the information in the routing table to determine the necessary routes. The results are used to populate the forwarding table. When packets arrive at a node, the node consults the forwarding table to determine where to send the packet.

The networks considered here rely primarily on airborne platforms flying in formation. In a combat situation we expect that the formation will frequently break with nodes coming in and out of radio (i.e., *node churn*). Routing protocols that are designed for this type of topology dynamics can be classified as *proactive* or *reactive* protocols.

Proactive protocols, such as DSDV periodically update the routing tables [8]. In contrast, reactive protocols (e.g. DSR and AODV) update the routing tables only when routes need to be created or adjusted due to changes to topology [8]. Proactive protocols are in general better at providing QoS guarantees for real-time traffic such as multimedia. Their disadvantage lies in the traffic volume overhead generated by the protocol

itself. Reactive protocols scale better than proactive protocols, but will experience higher latency when setting up a new route [8].

For additional and more in-depth information about these topics you may consult [8]–[10].





# CHAPTER 3

## Conceptual architecture

---

The proposed architecture for the COM stack is shown in Figure 3.1. There are several architectural entities with whom the COM stack interfaces with or is affected by: mission computer (MC), resource manager (RM), EW stack and waveform scheduler.

The RM allocates CPU and AESA resources to EW, COM and waveform scheduler. There is no direct interaction between RM and the COM stack. From COM's perspective, the outcome of the management is that resources needed by COM are granted or revoked.

The MC is a device pre-configured with mission parameters such flight path, encryption keys, COM and EW settings. The MC communicates with the COM stack through an interface referred to as IP\_MC. The other end of the interface is located within the COM stack and is called IP\_ETH. The RM forwards data between the two interfaces.

Communication with and control of the electronic warfare systems is managed by the EW stack. In the context of this project, the EW stack is a black box. There is no communication between the EW stack and the COM stack. EW always preempts COM on resource usage, having RM temporarily drain available COM resources. This may cause data in COM to become stale. This means that all COM payloads need to be timestamped so that a receiving COM stack can decide if the data is still fresh (i.e., useable) or not (i.e., should be discarded).

The COM and EW stack output each a bitstream referred to as waveform. The task of the waveform scheduler is to interleave the EW and COM waveforms for over-the-air (OTA) transmission. From the perspective of the COM stack, the waveform scheduler is a black box.

The remainder of this section will focus on COM stack. Its main purpose is to exchange user data. This includes data from the MC, such as situation awareness (SA) data (e.g., geodetic position, heading, air speed), sensor information (e.g., bi-static radar data) and other aircraft status and tactical data. It may also include pilot voice communication encoded with a mixed-excitation linear prediction (MELP) codec [11] and encapsulated within real-time transport protocol (RTP) packets [12]<sup>1</sup>. In this case, the capacity needs to be reserved within the network to guarantee the logical channel since voice always has high priority. Finally, the COM data may include signaling traffic, such as channel estimates, employed forward-error correction (FEC), and modulation.

---

<sup>1</sup>RTP makes use of UDP.

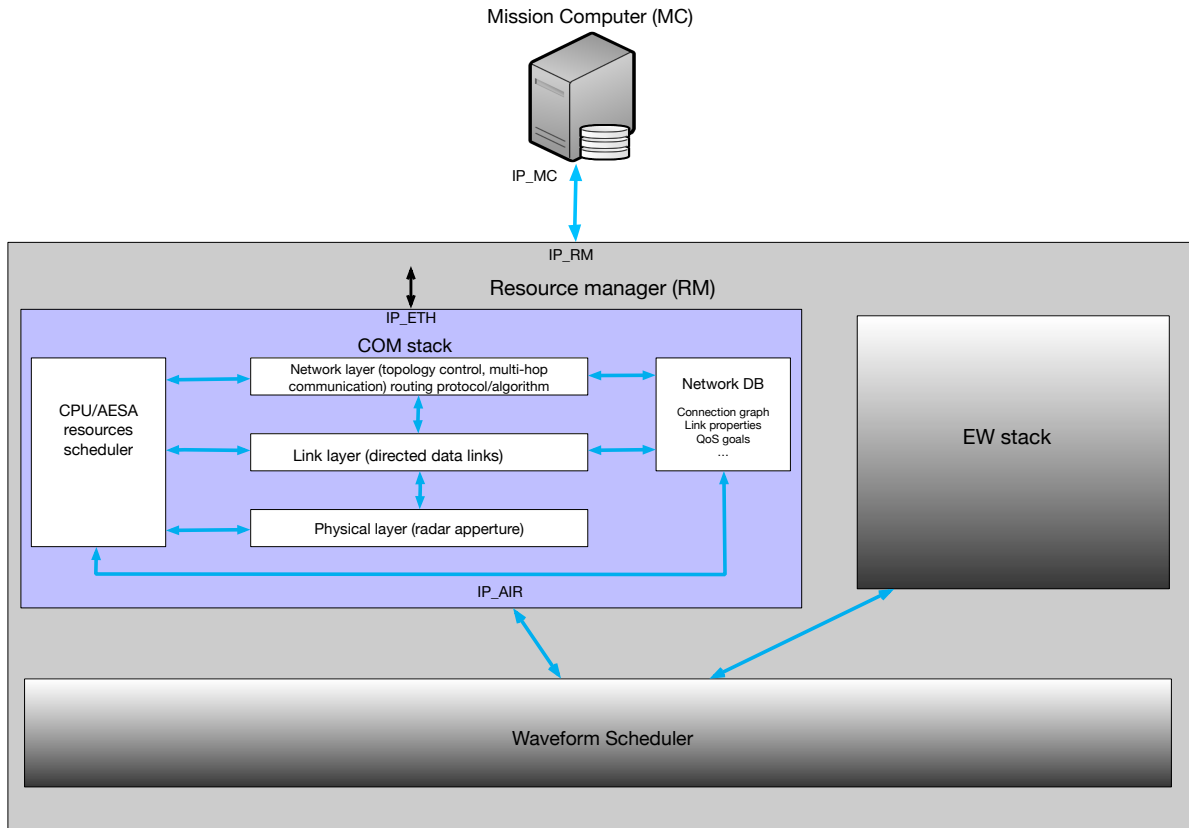


Figure 3.1: Conceptual architecture

## 3.1 Physical layer

The physical layer is responsible computing the waveform for OTA transmission. The OTA transmission and reception is performed with the help of a software-defined radio (SDR) system. A waveform in this context denotes all transformations such as modulation, channel encoding and filtering that are applied to information in order to convert it to a radio signal that can be transmitted. Receivers apply corresponding transformations to the signal in order to convert it back to information. As an example, the Joint Tactical Radio System (JTRS) wideband network waveform (WNF) can combine orthogonal frequency-division multiplexing (OFDM) with frequency hopping and forward error correction (FEC) [13].

In a sense, "physical layer" is a misnomer since the waveform computation is performed by software executing on general purpose processors potentially offloading some of the functionality to dedicated field-programmable gateway arrays (FPGAs) and digital signal processors (DSPs).

When transmitting, the input to the physical layer comes as frames from the link layer. The frames are processed according to the selected waveform and the output is a bitstream also referred to as waveform. Thus, depending on the context, "waveform" refers either to the type of transformations applied to frames or to the output of a set

of such transformations. The output waveform is sent to the waveform scheduler to be interleaved with the waveform outputted by the EW stack.

When receiving, the RM arranges for the received waveform (bitstream) from the AESA antennas to arrive as input to the physical layer. This input is processed into complete frames that are passed to the link layer.

## 3.2 Link layer – Ethernet II

The link layer interfaces with the physical layer to create the abstraction of a point-to-point (unicast) communication channel (i.e., a link).

By default, the link layer will have access to two interfaces:

- IP\_ETH, used for communicating with the MC
- IP\_AIR, used for OTA communication with other platforms (airborne or on the ground)

The interface, links and associated subnets are shown in Fig. 3.2.

Outgoing data coming as input from the network layer is encapsulated inside common Ethernet II frames [14], and then handed over to the physical layer. Incoming frames from the physical layer are decapsulated and the extracted payload is passed to the network layer.

The Ethernet II frames can carry payload data in the size 46–1500 bytes.

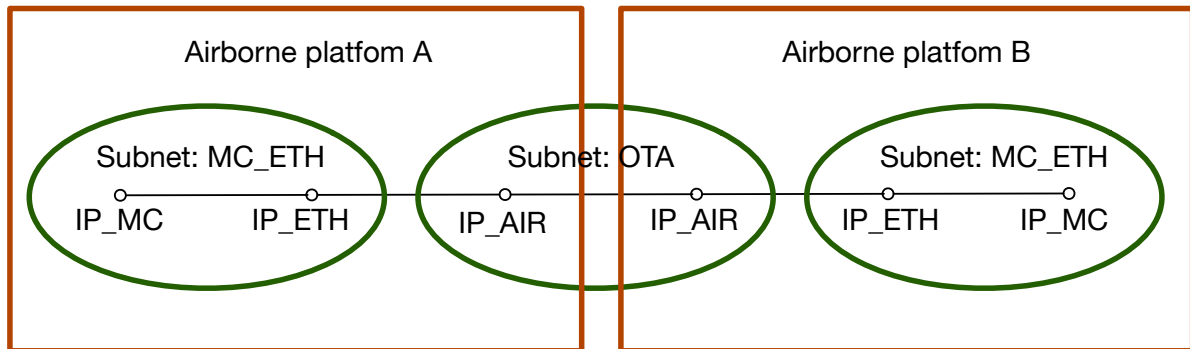


Figure 3.2: Network architecture

## 3.3 Network Layer – IPv4

The network layer interfaces with the link layer to enable data transport over multiple links, so called multi-hop routing. The implementation will be that of a standard IPv4 link layer. IPv6 will not be used.

Outgoing traffic comes from a standard transport layer (not shown in Fig. 3.1) as either UDP or TCP packets. Each packet is encapsulated into an IPv4 datagram and passed to the link layer. Similarly, received IP datagrams are decapsulated and the TCP or UDP payload is passed to the transport layer.

Only standard headers will be used, which means the IP Options field and the TCP Options field will not be present. Consequently, the size of the TCP/IP and UDP/IP headers will be 40 and 28 bytes, respectively. Header compression may be used for UDP/IP to reduce the header size to 20 bytes.

The default maximum transfer unit (MTU) size for Ethernet is 1500 bytes, which implicitly also applies to UDP traffic. Since the TCP Options field is not used, the default maximum segment size (MSS) size for TCP (536 bytes) will be used. This means that the TCP MTU will be reduced to 576 bytes (MSS plus TCP/IP headers size).

Depending on the physical layer technology, the above MTU may be too large. In this case IP fragmentation may occur to accommodate the smaller MTU. If fragmentation is not allowed, then IP datagrams exceeding the MTU will be dropped. Optionally, path MTU discovery can be employed to learn the smallest MTU on the path to a specific destination.

Standard Internet Control Message Protocol (ICMP) will be used for diagnostic and error notification.

Similarly, standard Address Resolution Protocol (ARP) will be used over the IP\_ETH interface to lookup the Ethernet MAC address corresponding to an IPv4 address. It is desirable to forego the use of ARP over the IP\_AIR interface, for example, by statically mapping the last 3 bytes of the MAC address to the last 3 bytes of IP address assigned to the same interface. This assumes that the MAC address is configurable.

## 3.4 Multicast and broadcast

Conventional multicast and broadcast data communication lays on the assumption of a shared medium. When a packet is sent over the medium, the packet is received by all interfaces connected to the medium as long as signal strength has not decreased beyond the minimum level required to decode the packet. For radio networks this assumption holds when an omnidirectional antenna is used.

However, with directional antennas only nodes in specific directions are targeted for communication. Often, the other remaining nodes will not be able to receive the data.

A solution to this problem is to resend the packet in multiple directions (e.g., toward each node) in order to ensure all nodes in the network receive the data. This will maintain compatibility with multicast applications, although less efficiently than in the case of shared medium in terms of amount of transmitted data.

# CHAPTER 4

## Use cases

---

### 4.1 Situation awareness data

A fundamental aspect of our proposed protocol is that we have access to data that are referred to as *situation awareness (SA) data*. Situation awareness is a critical component in military command and control operations, including flight missions in combat situations. In order to make real-time decisions about tactical maneuvers during a combat flight mission, the pilots must have good and accurate information about both adversary and friendly aircraft. SA data contain such information.

In our proposed solution, we work with a three-dimensional Euclidean space. The SA data consist of the following:

- The  $x$ -position (longitude),  $y$ -position (latitude) and  $z$ -position (altitude) of each friendly aircraft in the current situation;
- The speed in the  $x$ -,  $y$ -, and  $z$ -directions of each friendly aircraft in the current situation;
- The acceleration in the  $x$ -,  $y$ -, and  $z$ -directions of each friendly aircraft in the current situation;
- The  $x$ -,  $y$ -, and  $z$ -positions of each adversary aircraft in the current situation;
- The speed in the  $x$ -,  $y$ -, and  $z$ -directions of each adversary aircraft in the current situation;
- The acceleration in the  $x$ -,  $y$ -, and  $z$ -directions of each adversary aircraft in the current situation.

In some cases, the SA data only contain incomplete information regarding adversary aircraft position, usually the bearing (i.e. direction) from own aircraft location. This may be sufficient in our case, but otherwise the range (or distance) may be estimated with some uncertainty, e.g., by triangulation of a number of different observations.

In our work, a node has two sources of SA data. The first one is the set of SA sensors integrated with the airborne platform. The sensors have a maximum operational range, outside of which they cannot work reliably. We refer to the acquired sensor data as *local SA data*. The union of all friendly nodes' local SA data is the totality of environmental knowledge that friendly nodes pose as a group. We refer to this as a *unified SA view*. It is important to keep in mind that although the unified SA view contains more data than

available for a single node, it does not provide total SA visibility. Some nodes, friendly or otherwise, can be located so far away that they are not captured in the local SA data of any of the friendly nodes and are thus not available in the unified SA view. Each friendly node strives to obtain the unified SA view through exchange of SA data with friendly nodes. This is the second source of SA data. A node that receives SA data from another friendly node merges that with its own local SA and with previously received SA data from other nodes into something called the *node's SA view*. The merging operation favors local SA data over received SA data. In the ideal case, the node's SA view becomes identical to the unified SA view. However, due to latency, packet loss and nodes out of range, a node's SA view may diverge from the unified SA view. When this happens, it prevents the nodes from converging on a common topological view [9]. This phenomenon can lead to suboptimal routing and strategies should be put in place to alleviate its effects.

The local SA data are updated regularly, and each SA datum has a timestamp. However, how often the SA data are updated is not completely defined. The SA data are used to keep track of where all aircraft are at each time. Accordingly, since the SA data are updated at certain intervals, the local aircraft needs to update the positions of the other aircraft in the interval  $t_i$  to  $t_{i+1}$ , where  $\delta = t_{i+1} - t_i$  is the interval between updates/exchanges of the SA data.

Based on the SA data, we know the position of all friendly as well as adversary aircraft. In the next step, we can then calculate in which directions we can transmit using directional antennas in order to reach each aircraft directly, provided they are in range to receive the radio signal (Tx range). Further, we can also calculate whether other aircraft are reachable through intermediate friendly nodes, thus enabling a multi-hop routing protocol. The position of adversary aircraft allows us to determine if we would leak packets if transmitting towards a specific node. When using directional antennas, the radiation pattern will include a main lobe and a set of sidelobes. The region of 3D space where the signal can be detected, through the either main lobe or sidelobes, is referred to as a *forbidden sector*, as described in Section 5.1. HDARP avoids leaking packets by selecting routes outside forbidden sectors if such routes are available.

An important aspect of the topology control and routing scheme is that aircraft can both enter and leave a configuration. The enter/leave information should be present in the situation awareness data, thus enabling the routing information to be updated with new/disappearing nodes (aircraft).

## 4.2 Example use cases

One of the main advantages of a directional antenna is that it transmits only in a narrow angle, for example 10 degrees, which reduces the possibility of adversary detection. Therefore, we need to design a routing protocol that avoids transmitting in a direction where an adversary aircraft is located, which we call a *forbidden direction*. The forbidden direction is assumed to be aligned with the antenna boresight. By combining

the forbidden direction with information about the shape of main lobe and sidelobes of radiation pattern one can specify the associated forbidden sector. The calculation of forbidden direction and sector and, thus, which aircraft we can communicate with in a single-hop, is an important part of the developed routing protocol.

Figure 4.3 shows a use case where an adversary aircraft is in the neighborhood. In this case, when A wants to communicate with B, A is forced to use multi-hop via C in order to reach B without risk of being detected.

In order to describe the topology control and the routing protocol, we will start with the use cases below. In the evaluation of the protocol, we have more complex use cases (scenarios) as outlined in Section 6.3.

- A new aircraft enters the network. This use case can be broken down into
  - (i) two aircraft establishing connection with each other, as in Figure 4.1, and
  - (ii) a new aircraft enters an existing network with  $N$  aircraft.
- An aircraft loses contact with the network. This use case can be broken down into
  - (i) an aircraft acting as an end node (e.g., “C” in Figure 4.2) loses contact with the other ones in a network of  $N$  aircraft, which does not affect the routing between the other  $N - 1$  nodes, and
  - (ii) an aircraft acting as a relay node (e.g., “B” in Figure 4.2) loses contact with the other ones in a network of  $N$  aircraft, which affects the communication and network topology between the other nodes.
- Two friendly aircraft communicating with each other; see Figure 4.1.
- Three friendly aircraft communicating with each other, using both single-hop routing ( $A \leftrightarrow B$  and  $B \leftrightarrow C$ ) and multi-hop routing ( $A \Rightarrow B \Rightarrow C$ ); see Figure 4.2.
- Three friendly aircraft communicating with each other but with an adversary aircraft in the neighborhood. Since the adversary aircraft is in the send direction  $A \Rightarrow B$ , we are forced to use multi-hop routing  $A \Rightarrow C \Rightarrow B$  when A wants to communicate with B; see Figure 4.3.



Figure 4.1: Two friendly aircraft communicating with each other

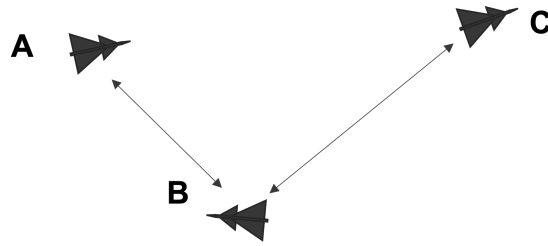


Figure 4.2: Three friendly aircraft communicating with each other, using both single-hop routing and multi-hop routing

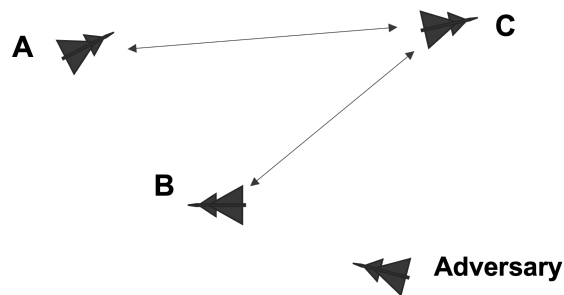


Figure 4.3: Three friendly aircraft communicating with each other, but with an adversary nearby forcing multi-hop routing to be used



# CHAPTER 5

## HDARP

---

Each node participating in the FANET runs an instance of the routing protocol described in Algorithms 1–4. It is assumed that each node is equipped with a mission computer (MC), which contains parameters pre-configured before the start of a mission. Examples of pre-configured parameters may include the node identification, identification of participants in the same squadron, MAC addresses assigned to network interfaces and corresponding IP addresses for all members of squadron, configured cryptographic services and associated cryptographic material, etc. This information is integrated into the node's SA view.

When the routing protocol is started, it will begin the bootstrapping procedure described in Algorithm 1. The first step is to interface with the aircraft sensors and on-board auxiliary systems to identify any other nodes, friends or adversaries detectable in the range of the sensors. The information will include the position, velocity and acceleration of the discovered nodes, essentially yielding the node local SA data mentioned in Section 4.1. The local SA data are inserted into the node's SA view, which is an aggregation of SA data from local sensors and SA data obtained from other friendly nodes through routing protocol message exchanges. In bootstrap mode, no such exchanges have taken place yet, and therefore, the node's SA view contains only local SA data. The third step is to call the HDA\_ROUTING procedure (Algorithm 4) to compute routes to any of the friendly nodes discovered. Finally, a timer called *send\_SA\_update* is configured. When this timer expires, the node will share its SA view with other nodes located one hop away, which is the procedure outlined in Algorithm 2.

---

**Algorithm 1** Bootstrap at node  $n$ .

---

**Require:** Identity of node  $n$  running the bootstrap

- 1: Use aircraft sensors to collect SA data (*local\_SA*)
  - 2: Insert *local\_SA* into *SA\_view*
  - 3: HDA\_ROUTING(*SA\_view*,  $n$ ) ▷ Executes Algorithm 4
  - 4: Schedule *send\_SA\_update* timer ▷ Triggers Algorithm 2 when it expires
- 

Algorithm 2 is rather straightforward. When the *send\_SA\_update* timer expires, this algorithm is invoked, and during its execution, it will prepare a message containing the node's SA view and send it to the one-hop friendly neighbors. Information from the MC is not included in the updates, since it is assumed that each node has access to it from their own MC. After that, it will re-schedule the *send\_SA\_update* timer for the next update to the neighbor nodes.

---

**Algorithm 2** Update neighbor nodes.

---

**Require:**  $SA\_view$ , identity of node  $n$  running the algorithm

```

1: procedure SEND_SA_UPDATE( $SA\_view, n$ )
2:   for each friendly node  $dst$  in  $SA\_view$  reachable in one hop do
3:     Transmit  $SA\_view$  to  $dst$ 
4:   end for
5:   Schedule  $send\_SA\_update$  timer            $\triangleright$  Triggers this algorithm when it expires
6: end procedure

```

---

Algorithm 3 handles the situation when an SA view is received from a friendly neighbor. First, the node will update its local SA data by interfacing with the aircraft sensors and on-board auxiliary systems. If the new local SA data conflict with data in the node's SA view, for example with SA data received earlier from a friendly node, the information from the local SA data will replace the existing data in the SA view. Our policy is that fresh local SA data are trusted above anything else. The currently received SA view,  $recvd\_SA\_view$ , is merged into the node's SA view using the same policy. Since SA data are timestamped, entries from the  $recvd\_SA\_view$  will replace the node's existing SA view data only if newer. The final step is to call the HDA\_ROUTING procedure (Algorithm 4) to re-compute routes that were affected by the received  $recvd\_SA\_view$  message or changes in the node's local SA data.

---

**Algorithm 3** SA fusion at node  $n$ .

---

**Require:**  $SA\_view$ , received  $SA\_view$  from neighbor, node  $n$  running the algorithm  
 $\triangleright$  Triggered by message reception

```

1: procedure RECEIVED_SA_UPDATE( $SA\_view, recvd\_SA\_view, n$ )
2:   Use aircraft sensors to collect fresh SA data ( $local\_SA$ )
3:   Merge  $local\_SA$  into existing  $SA\_view$             $\triangleright$   $local\_SA$  data are preferred
4:   Merge  $recvd\_SA\_view$  into  $SA\_view$             $\triangleright$   $local\_SA$  data are preferred
5:   HDA_ROUTING( $SA\_view, n$ )                      $\triangleright$  Executes Algorithm 4
6: end procedure

```

---

The aim of the HDARP routing protocol described in Algorithm 4 is to exploit the information from the node's SA view to determine the shortest paths from the node to all other friendly nodes, while avoiding forbidden sectors. The actual shortest-path computation is performed using an adaptation of Dijkstra's shortest-path algorithm [15] that produces a shortest-path tree. This approach is well known in computer networking, and therefore, rather than explaining it here, we point the interested reader to [9], [16].

Dijkstra's algorithm requires as input the source node for all the paths to be produced (denoted by  $n$  in the algorithm) and a weighted graph  $\mathcal{G}$  consisting of all vertices and directed edges in the graph, which in our case correspond to nodes and links. When directed edges are used in a graph, the edge  $(u, v)$  is distinct from  $(v, u)$ .

The first step in Algorithm 4 is to collect all friendly nodes from the SA view into the set  $\mathcal{F}$ . Secondly, we create an empty set  $\mathcal{L}$  that will eventually be populated with links

connecting a pair of nodes. We cannot add the links yet because we need to determine *a)* which pairs of nodes are connected by a link and *b)* the weight (cost) assigned to that link. Two nodes,  $u$  and  $v$ , will be connected by a link  $(u, v)$  if node  $v$  is in Tx range from  $u$ . In addition, if node  $u$  is in Tx range from  $v$ , there will be an additional link  $(v, u)$ . The weight of a link is determined by whether or not the link connecting the two nodes overlaps with a forbidden sector. To enable this determination, we collect all adversary nodes from the SA view into the set  $\mathcal{A}$ .

The algorithm iterates through each node  $src$  in  $\mathcal{F}$  and creates an outgoing link to each of the remaining  $dst$  nodes that can be connected to it according to *a)* and *b)*. If a link was created, the algorithm will iterate through each adversary node  $a$  in  $\mathcal{A}$  to test if it causes a forbidden sector for the new link. The forbidden sector detection is performed as described in Section 5.1. Links outside a forbidden sector are assigned unit cost, whereas links inside a forbidden sector are penalized with a high cost. The link can be excluded from the topology instead of increasing its cost if the mission requires radio silence. The costs along a path are additive. Dijkstra's algorithm will attempt to minimize the total cost of a path towards a specific destination.

In a network with  $n$  nodes, the longest possible acyclic path consists of  $n - 1$  links. If all links are outside forbidden sectors, the cost for such a path is  $n - 1$  considering the unit link cost as mentioned above. Thus, the lowest penalty cost that can be chosen for links inside forbidden sectors is  $n$ , the number of nodes in the network. A path consisting of one or more such links will have a cost that exceeds the cost of any acyclic path where all links are outside forbidden sectors. In our simulations, the nodes forward IPv4 packets. The time-to-live (TTL) field in the IPv4 header is 8-bit wide, limiting the longest path to 255 links. Therefore, the lowest penalty cost for IPv4 links is 256. In our case, we have set the cost of links located in forbidden sectors to 5000. This value does not confer any advantage or disadvantage compared with 256, but is rarely occurring in the simulations and is thus easy to find in the log files.

In the final part of Algorithm 4, the shortest-path tree produced by Dijkstra's algorithm will be used to update the IPv4 routing tables of node  $n$ .

## 5.1 Forbidden Sector Detection

The goal of the forbidden sector detection method is to determine if an adversary aircraft can detect the communication between two friendly nodes. More specifically, it is to determine if the adversary is able to distinguish the main lobe or sidelobes of the incoming signal from electromagnetic noise. To do so, we construct a 3D geometrical model (i.e., a 3D volume) of the radiation pattern, main lobe and sidelobes combined and determine if any of the adversary aircraft are located within the volume. If any such adversaries are found, then the sending node should avoid direct communication and instead try to forward the packet through other friendly nodes unaffected by forbidden sectors.

We have used a tetrahedron as a first-order approximation of the radiation pattern, as shown in Figure 5.1. This provides us with an acceptable tradeoff between accuracy and

---

**Algorithm 4** Hostile-Direction Aware Routing (HDARP) at node  $n$ .

---

**Require:**  $SA\_view$ , node  $n$  running the algorithm

```

1: procedure HDA_ROUTING( $SA\_view, n$ )
2:   Group friendly nodes from  $SA\_view$  in a set  $\mathcal{F}$ 
3:   Create an empty set  $\mathcal{L}$  that will store links between friendly nodes
4:   Group remaining nodes from  $SA\_view$  in a set  $\mathcal{A}$ 
5:   Use the sets  $\mathcal{F}$  and  $\mathcal{L}$  to define a directed topology graph  $\mathcal{G}(\mathcal{F}, \mathcal{L})$ 
6:   for each node  $src \in \mathcal{F}$  do
7:     for each node  $dst \in \mathcal{F}$  other than  $src$  do
8:       if  $dst$  in Tx range from  $src$  then
9:         Add the directed link  $(src, dst)$  to set  $\mathcal{L}$ 
10:        Set link cost:  $(src, dst).weight \leftarrow 1$ 
11:      else
12:        continue
13:      end if
14:       $f \leftarrow \text{IS\_FORBIDDEN\_SECTOR}(src, dst, \mathcal{A})$ 
15:      if  $f = \text{True}$  then
16:        Set link cost:  $(src, dst).weight \leftarrow 5000$ 
17:        break
18:      end if
19:    end for
20:  end for
21:   $SPT \leftarrow \text{DIJKSTRA}(n, \mathcal{G}(\mathcal{F}, \mathcal{L})) \quad \triangleright \text{Shortest paths from } n \text{ to other nodes in } \mathcal{F}$ 
22:  Use  $SPT$  to update the IPv4 routing table entries at  $n$ 
23: end procedure

```

---

computation time: the last one being particularly important for reducing simulation time. The tetrahedron is created such that the sender is at the center of the tetrahedron base, and the receiver, Blue 2, is located at the apex of the main lobe. Obviously, this assumes that the receiver is within Tx range from the sender; otherwise, direct communication is not possible. In addition, we assume that when the receiver is located closer than Tx range, the sender can adjust the transmission power so the SNR for received signal is just enough for the sender to decode the data. This reduces the likelihood of leaking data behind the receiver. However, according to information from our aerospace industry partner, the receiver can decode the incoming signal (with an acceptable BER) if its SNR is at least 10 dB. Furthermore, given that a signal can be *detected* if it is just above the noise floor, when this information is plugged into a simplified path loss model [17], the outcome indicates that a signal can be discerned as far as three times the distance from sender to receiver along antenna boresight. Therefore, we extend the tetrahedron apex at three times the distance from the sender and receiver, which is the *detection range*, the maximum distance at which an adversary can detect the transmission. Similarly, we extend the radius of the tetrahedron base (i.e., the distance from center to each of the three vertices) to 1/30 of the detection range to prevent detection through the sidelobes.

Thus, our forbidden sector detector consists of the tetrahedron constructed as described above combined with logic to detect if any adversary is located with the 3D space of the tetrahedron.

It is important to point out that when the transmission power is adjusted for the distance to the receiver, the volume of 3D space used by main and side lobes of the signal will change accordingly. Similarly, the tetrahedron is scaled proportionally to the distance to the receiver, but the aspect will remain the same.

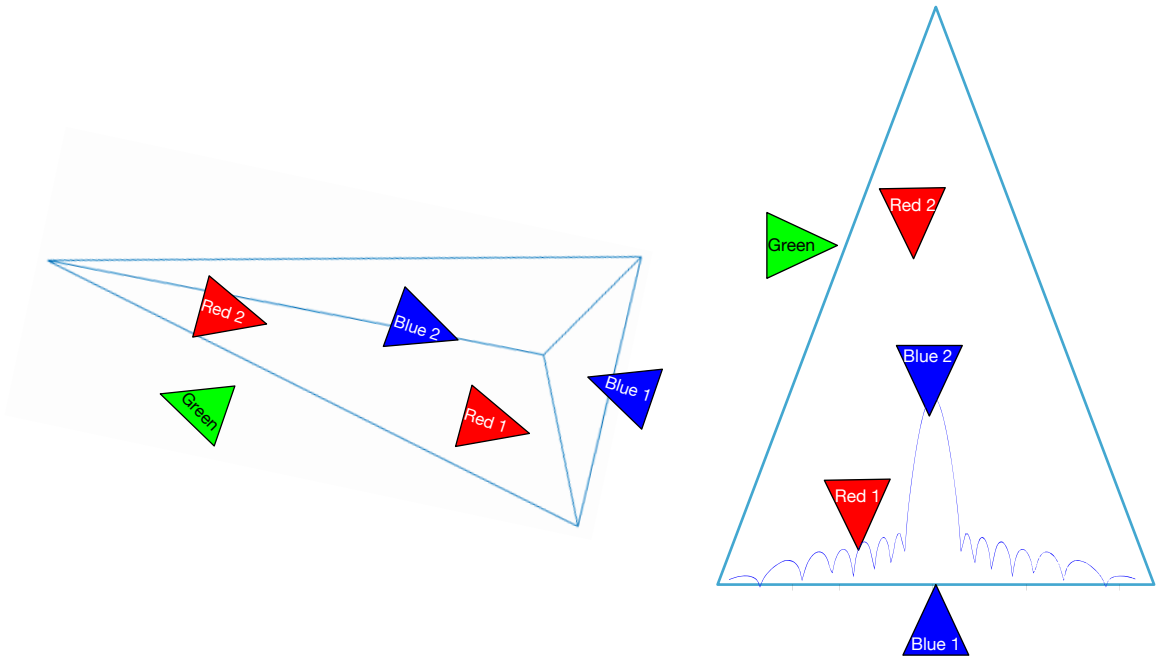


Figure 5.1: Forbidden sector detection. To the left: 3D view of detector operation. To the right: cross-section of 3D radiation pattern with detector. Ratio between size of main lobe and size of sidelobes is decreased on purpose in order for the sidelobes to be visible in the figure.

The left part of Figure 5.1 illustrates the operation of the detector in the scenario where node Blue 1 wants to transmit to node Blue 2. The red and green nodes are hostile nodes that should not be able to detect the transmission. The right part of Figure 5.1 represents a cross-section of the figure on the left, as seen from above, and is rotated so that the tetrahedron apex points upwards. The figure also shows the embedded radiation pattern (also a cross-section of the 3D pattern). The Green node is outside the tetrahedron and thus does not pose a detection risk. However, node Red 1 is able to detect the signal from the sidelobes. In addition, although the signal that passes Blue 2 has a very low SNR, it is also detectable by Red 2. Thus, the location of either Red 1 or Red 2 is enough reason to conclude that the transmission from Blue 1 to Blue 2 is located inside a forbidden sector and that an alternative path through an intermediate friendly node would be preferred.

The logic used to detect if an adversary is inside the tetrahedron is captured by Algorithms 5–7<sup>1</sup>. Algorithm 5 constructs a tetrahedron with the apex oriented towards the destination node and with the sender node located at the center of the base. We use the convention that  $T.v1$ ,  $T.v2$  and  $T.v3$  are the coordinates for the three vertices defining the base of the tetrahedron  $T$ . The position of the tetrahedron apex (forth vertex) is available in  $T.v4$ .

---

**Algorithm 5** Forbidden sector detection.

---

**Require:** sender, receiver, set of adversary nodes

```

1: procedure IS_FORBIDDEN_SECTOR( $src$ ,  $dst$ ,  $\mathcal{A}$ )
2:    $T \leftarrow \text{TETRAHEDRON}(src.pos, dst.pos)$ 
3:   for each node  $a \in \mathcal{A}$  do
4:     if ISINSIDE( $T$ ,  $a$ ) = True then
5:       return True
6:     end if
7:   end for
8:   return False
9: end procedure

```

---

The attribute `pos` appearing to the right of a node variable (e.g.,  $src$  and  $dst$ ) contains the 3D coordinates of that node. The algorithm iterates through all adversary nodes, calling the `ISINSIDE` procedure (Algorithm 6) to check if any generate a forbidden sector. In that case, the algorithm aborts and returns **True**. Otherwise, if none of the adversaries are located within the tetrahedron space, the algorithm returns **False**.

Algorithm 6 checks for each of the four planes making up the tetrahedron if the opposite vertex and the adversary node are located on the same side of the plane. If this is true for all planes, it means that the position of the adversary is a point located inside the tetrahedron. Otherwise, the adversary is on the outside.

The logic to detect if the opposite vertex and the adversary are located on the same side of a plane is shown in Algorithm 7. The first three input parameters,  $\mathbf{p}$ ,  $\mathbf{q}$  and  $\mathbf{r}$ , are the coordinates of the vertices defining the plane. Vertex  $\mathbf{p}$  is used as common origin when using the coordinates to construct two vectors,  $\mathbf{q} - \mathbf{p}$  and  $\mathbf{r} - \mathbf{p}$ , that span the plane. The cross-product  $\mathbf{n}$  of these two vectors is perpendicular to the two vectors spanning the plane, and is thus a normal to the plane. Similarly, we use the remaining two parameters  $\mathbf{v}$  and  $\mathbf{a}$  to construct two vectors  $\mathbf{v} - \mathbf{p}$  and  $\mathbf{a} - \mathbf{p}$ , using the same origin  $\mathbf{p}$  as before. The normal  $\mathbf{n}$  is then used as a reference direction when computing the dot products of the normal with these two vectors. The dot product returns a positive value if the angle  $\theta$  between the vector and normal is  $-\pi < \theta < \pi$  and it returns a negative value when  $\pi < \theta < 3\pi$ . When the vector and normal are perpendicular their dot product is zero. Therefore, if both dot products,  $d1$  and  $d2$ , have the same sign,

---

<sup>1</sup>The algorithms presented here are based to a large extent on discussions available online at <https://stackoverflow.com/questions/25179693/how-to-check-whether-the-point-is-in-the-tetrahedron-or-not>.

---

**Algorithm 6** Check if adversary is within tetrahedron.

---

**Require:** tetrahedron, adversary node

```

1: procedure IS_INSIDE( $T, a$ )
2:    $p1 \leftarrow \text{IS\_ON\_SAME\_PLANE\_SIDE}(T.v1, T.v2, T.v3, T.v4, a.pos)$ 
3:    $p2 \leftarrow \text{IS\_ON\_SAME\_PLANE\_SIDE}(T.v2, T.v3, T.v4, T.v1, a.pos)$ 
4:    $p3 \leftarrow \text{IS\_ON\_SAME\_PLANE\_SIDE}(T.v3, T.v4, T.v1, T.v2, a.pos)$ 
5:    $p4 \leftarrow \text{IS\_ON\_SAME\_PLANE\_SIDE}(T.v4, T.v1, T.v2, T.v3, a.pos)$ 
6:   if  $p1 = \text{True}$  and  $p2 = \text{True}$  and  $p3 = \text{True}$  and  $p4 = \text{True}$  then
7:     return True
8:   else
9:     return False
10:  end if
11: end procedure

```

---

it means that  $\mathbf{v}$  and  $\mathbf{a}$  are on the same side of the plane. When both dot products are zero, it means that the two vectors are on the plane. In this situation, we still claim the two vectors are on the same side as this weighs towards concluding that the adversary is within the tetrahedron space (pessimistic view). The SIGN function shown in Algorithm 7 returns integer -1 if the numeric argument is negative, +1 if positive, and 0 otherwise.

---

**Algorithm 7** Check if opposite vertex and adversary are on the same side of the tetrahedron plane.

---

**Require:** Tetrahedron plane vertices, opposite vertex, adversary position

```

1: procedure IS_ON_SAME_PLANE_SIDE( $\mathbf{p}, \mathbf{q}, \mathbf{r}, \mathbf{v}, \mathbf{a}$ )
2:   Compute normal to the plane spawned by  $\mathbf{q} - \mathbf{p}$  and  $\mathbf{r} - \mathbf{p}$ :
3:    $\mathbf{n} \leftarrow (\mathbf{q} - \mathbf{p}) \times (\mathbf{r} - \mathbf{p})$   $\triangleright$  Cross-product
4:   Compute dot products between plane normal and vectors towards  $\mathbf{v}$  and  $\mathbf{a}$ :
5:    $d1 \leftarrow \mathbf{n} \cdot (\mathbf{v} - \mathbf{p})$ 
6:    $d2 \leftarrow \mathbf{n} \cdot (\mathbf{a} - \mathbf{p})$ 
7:   if  $\text{SIGN}(d1) = \text{SIGN}(d2)$  then
8:     return True
9:   else
10:    return False
11:  end if
12: end procedure

```

---





# CHAPTER 6

## Simulation framework

---

We have used the OMNEST simulator framework to evaluate HDARP<sup>1</sup>. OMNEST uses a modular, component-based approach to build simulations. At the core, OMNEST modules are written in C++, but at a higher level, they can be combined and extended using OMNEST's Network Description (NED) language. We also made use of the INETMANET [20] open-source model library, which contains models for the internet stack, wired and wireless link-layer protocols and more. Historically, INETMANET was forked from the official INET [21] model library in order to address the shortage of MANET protocol components. Nowadays, INET and INETMANET are pretty much aligned in terms of functionality and compatibility with each other. However, INETMANET continues to provide access to additional MANET protocols, which is the reason we preferred it for our study. INETMANET does not have specific versioned releases. The code we use in our simulations comes from Git commit 6708b98344e5fd5a5e788da97367efa9150629a2. Both INET and INETMANET are well described in [22].

We have compared HDARP's performance against five other MANET protocols available in INETMANET: AODV [23], BATMAN [24], DSDV [25], DSR-UU [26], and OLSR [27], respectively. Initially, we included additional MANET routing protocols from INETMANET, AODV-UU [28], Dymo [29], [30] and Dymo-FAU [31], but these crashed multiple times during our simulations and are therefore not included in the results. Notably, DSR-UU and AODV-UU are protocol implementations for the Linux kernel that later were also made operable with the ns-2 and OMNeT++ simulators.

For all nodes that are simulated, we used the NED language to inherit generic networking functionality from the AdHocHost component, which provides among other things a TCP/IP stack simulation model, support for mobility models, a loopback interface as well as a wireless interface. In addition, the nodes were configured to use one specific MANET routing protocol from the selection above, including our own HDARP routing protocol.

Every node derived from the AdHocHost component can be equipped with an arbitrary number of applications. These simulation modules exploit functionality of the underlying TCP/IP stack to communicate with peer modules application located on other nodes, typically using a socket abstraction. However, the applications can also subscribe for signals from lower layers and other modules, or hook into the functionality of the underlying TCP/IP stack to provide special processing for incoming and outgoing packets, much like the functionality of the Linux netfilter [32]. In our case, we equipped

---

<sup>1</sup>OMNEST is the commercial version of the well-known simulator framework OMNeT++ [18], [19]

the nodes in the simulation with two applications, `InterceptApp` and `UdpBasicApp`, described in Section 6.1 and Section 6.2, respectively.

The nodes were also equipped with a mobility model that imports realistic flight path traces provided by our aerospace industry partner. This module was implemented using a combination of C++ and NED. Our mobility model reads data from file where records are indexed by monotonically increasing timestamps. Each record contains the 3D position of a specific node at the time indicated by the timestamp. The module computes instantaneous node velocity and acceleration using the data from the records. In addition, the module interpolates the position of the aircraft between two consecutive timestamps using the computed velocity. The module emits a notification each time a node updates its position, either through interpolation or by advancing to the next record in the data. It is important to note that each node participating in the simulation is equipped with its own mobility model instance that emits notifications for that particular node.

HDARP nodes are configured as above with the notable exception that they require an additional SA module to implement situation awareness. Every HDARP node has its own SA module instance that subscribes to mobility notifications from all nodes in the simulation. The mobility data are used to update the node's SA view. The SA module has logic to determine if specific nodes are "visible" based on sensor range, which is a configurable parameter. Invisible nodes are excluded from the node's SA view computed by the module. The same procedure is applied when receiving SA updates from friendly nodes.

The HDARP routing module receives a notification from the SA module every time the SA view is updated. For each notification, it determines whether routes must be recomputed as described in Chapter 5 above. To avoid stale routes, the HDARP module purges the existing routes in the IPv4 routing table before installing routes derived from the current SA view.

Unfortunately, there is almost no support for antenna arrays components with beam-forming in INET/INETMANET, with the notable exception of [33]. Furthermore, our interest was primarily in the behavior of the routing protocol, separated from the intricacies of the link layer and physical layer models. Consequently, we made a pragmatic simplification by configuring the wireless interface to use the `AckingWirelessInterface` module. This module contains two submodules: a unit disk radio (`UnitDiskRadio`) and a very simple MAC protocol (`AckingMac`).

The unit disk radio is configured to perform interference modeling, which means that when a node transmits a MAC frame, all nodes within Tx range will be able to receive the frame, unless other nodes within Tx range are transmitting at the same time, in which case the reception will fail. The model implies the use of a isotropic antenna, which is at odds with our aim to use directional antennas. Instead, we emulate the effects of a directional antenna through the `InterceptApp` module, which is presented in Section 6.1.

The `AckingMac` is trivial in the sense that it offers encapsulation and decapsulation of link layer frames, but no medium access procedure or retransmission.

For over-the-air tactical links, it is common practice to avoid the use of the Address

Resolution Protocol (ARP) [34] in order to reduce latency. Instead, IP addresses are mapped to MAC addresses in a static table available as a parameter in the MC, or the mapping is a deterministic function based on the assigned IP address of a node. We have configured the simulator to use GlobalArp in order to avoid ARP exchanges. The GlobalArp is a lookup table of IP to MAC address mappings available to all simulation nodes.

## 6.1 InterceptApp

The InterceptApp provides three services: it emulates the functionality of directional antennas for nodes derived from the AdHocHost component, it provides the means to measure the number of leaked packets by such nodes, and it helps implementing teams/groups (e.g., red, blue, green) while running a separate MANET for each team. To provide these services, InterceptApp uses a subset of the SA functionality from the SA module described above.

The application subscribes to notifications from the MAC layer about incoming packets received by the wireless network interface. Each notification provides access to the full packet, including the MAC headers. The InterceptApp extracts the source MAC address and the destination MAC address from the packet headers and uses these to look up the identification of the sender and receiver in the node's SA view. If the sender does not belong to the same team as the node that received the packet (i.e., the node where InterceptApp is currently executing) and directional antenna emulation is turned off, then InterceptApp will record the incoming packet as a leaked packet.

In the case when directional antenna emulation is enabled, the receiving node will run Algorithm 5 with sender and receiver identities as input for the first two parameters. The third parameter, the set  $\mathcal{A}$ , will contain a single element, which is the identity of the node that received the packet. In essence, the algorithm answers the following question: would this node have received the packet if the sender from the other team instead of isotropic antennas used directional antennas with a radiation pattern following the tetrahedron model? If the answer is yes, the received packet would be leaked even if directional antennas were in use, and thus, the packet is marked as leaked.

In either case (directional antenna emulation on or off), the application will force the TCP/IP stack to drop the packet if the sender belongs to a different team. Existing MANET protocol modules in INET/INETMANET are not aware of the concept of a team. Without InterceptApp, they will try and succeed to use nodes from other teams as relay nodes.

If the sender belongs to the same team, normal packet processing will ensue.

## 6.2 UdpBasicApp

As described above, all nodes in the simulation are equipped with an application called UdpBasicApp. The application can send UDP datagrams to a set of preconfigured IP addresses and port numbers. The datagram size and the send rate can be configured either as fixed values, or as random values drawn from a specific probability distribution. In addition, UdpBasicApp listens on a configurable port for incoming UDP datagrams and uses these to compute basic statistics for metrics such as throughput and packet lifetime.

We have configured UdpBasicApp to draw the datagram size from a discrete uniform distribution over the interval 100 bytes to 1000 bytes. Similarly, the datagram send rate follows a discrete uniform distribution over the interval 100 ms to 200 ms. This is intended as a rough approximation of low bitrate voice-over-IP communication between the planes, such as that produced by the Mixed Excitation Linear Prediction Enhanced (MELPe) codec, including real-time transport protocol (RTP/RTCP) headers [12], [35]. Each node in the simulation is configured to send UdpBasicApp datagrams only to all other nodes belonging to the same team, but none to nodes belonging to other teams.

The random numbers are generated using an implementation of the Mersenne Twister [36] pseudo-random number generator (PRNG) that is included in the OMNEST distribution. In OMNEST, multiple PRNG instances can run simultaneously to create independent streams of random numbers. We have dedicated a PRNG instance to the UdpBasicApp. This way, the random events in UdpBasicApp are not affected by random events in the reminder of the simulator (e.g., scheduled updates in the routing protocol that include a random delay component). The result is that the transmission time and size for UdpBasicApp datagrams remain the same when we change the routing protocol. In effect, this becomes the workload against which we evaluate the MANET protocols in this study.

## 6.3 Simulation Scenarios

In our evaluation of the protocols, we will use two different simulation scenarios:

- **Scenario 1:** R4B4, which contains four red aircraft and four blue aircraft representing two different teams (red and blue). This scenario is depicted to the left in Figure 6.1.
- **Scenario 2:** BVR (beyond visual range), which contains a total of 24 aircraft from three teams (red, blue, green). This scenario is depicted to the right in Figure 6.1.

In Scenario 1, the two teams start far enough from each other to avoid leaking packets to the adversary, but close enough (i.e., within Tx range) within the team to enable direct communication. The two teams approach each other until the majority of the nodes are in detection range from at least one of the adversary aircraft. At this point,

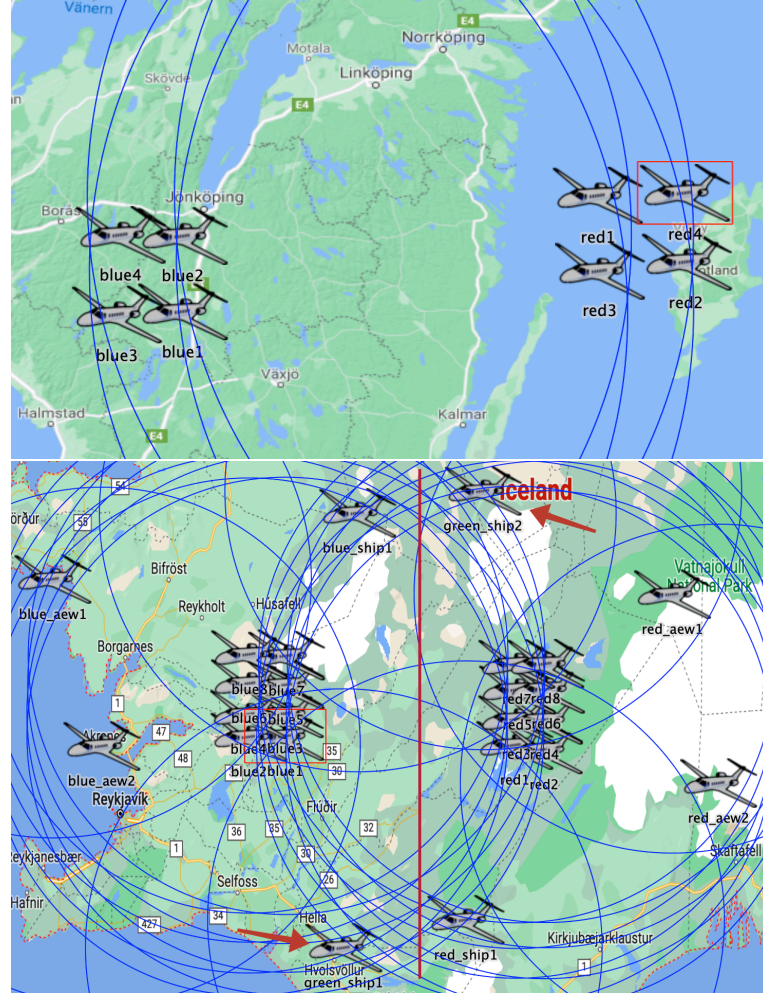


Figure 6.1: Simulation scenarios. Upper: Scenario 1. Lower: Scenario 2. Maps data: Google ©2023.

HDARP starts using multi-hop communication to avoid forbidden sectors. Eventually, the aircraft veer away from adversary nodes.

In Scenario 2, the red and blue team consist each of a bulk of eight fighter jets. These are shown closely packed together, visible as clusters in the figure. We have drawn a vertical red line in that figure that separates the two clusters. In addition, the red and blue teams have each two airborne early warning (AEW) nodes that act as command-and-control (C2) centers from behind the fighter jets. They are shown to the far left and right of the figure, respectively. Furthermore, the blue team has a node denoted as blue-ship1, visible at the top of the figure on the left side of the red vertical line. Similarly, the red team has a red-ship1 node located at the bottom, on the right side of the red vertical line. Blue-ship1 and red-ship play the role of mid-air tanker aircraft. The green team has two nodes, one at the top on the right of the vertical line and one at the bottom on left of the vertical line. We have drawn arrows in the figure to ease the identification of the green nodes in the figure.

The red and blue clusters are initially out of Tx range from each other, and thus, direct communication within the cluster is possible. The clusters approach each other while the AEW nodes remain behind. The tanker aircraft remain stationary through the whole simulation. When the two clusters come within Tx range, they begin using the tanker and AEW nodes in their team as relay nodes. The green nodes are out of Tx range for the entire simulation, and thus, cannot communicate with each other. Their role is to stress the directional antenna emulation part of the simulation, as well as the forbidden sector detection in HDARP. After a close encounter, the red and blue clusters return to their approximate starting positions.

In each scenario, we can choose one out of six routing protocols: AODV, BATMAN, DSDV, DSR-UU, HDARP (our protocol), and OLSR, respectively. A third parameter is the antenna type: directional (dir), or omnidirectional (omni). The choice of antenna only affects the operation of InterceptApp, but the simulation must be re-run if we want results for a different antenna type. To increase the statistical accuracy of the results, we run each scenario + protocol + antenna type combination 30 times with different RNG seeds.

## 6.4 Simulation Settings

In Table 6.1, we list the critical simulation parameters used to produce the results in this study. In the case where multiple parameter values were simulated, the distinct values are separated by comma in the Settings column. For the remainder of simulation components, including MANET protocols others then HDARP, we have used the configured default settings in OMNEST/INETMANET.

Table 6.1: Simulation settings.

Parameter	Settings	HDARP Specific	Description
Scenario	R4B4, BVR		Pre-recorded flight path traces.
Simulation duration	R4B4: 900 s, BVR: 1570 s		As obtained from our aerospace industry partner.
MANET protocols	ODV, BATMAN, DSDV, DSR-UU, HDARP, OLSR		Simulated MANET protocols, as available from INETMANET.
Antenna type	isotropic, emulated directional		Isotropic antennas are always used, but directional antenna emulation can be enabled via InterceptApp (see Section 6.1).
Tx range	300 km		Maximum antenna transmission range, where decoding is still possible.
Adjust TX power <sup>1</sup>	True		Adjust Tx power to destination range, as described in Section 5.1.
Link bitrate	10 Mbps		Effective bitrate for wireless interface.
ARP functionality	Global ARP		Over-the-air interfaces do not use ARP (see Section 3.3).
UdpBasicApp message length	intuniform (100, 1000)		Discrete uniform distribution for UDP datagram size (in bytes).
UdpBasicApp message interval	uniform (0.1, 0.2)		Continuous uniform distribution for time between consecutive UDP datagram transmissions (in seconds).
SA range	300 km	✓	SA sensor range.
SA max age	5 s	✓	Time before SA data received from peers is considered stale.
Forbidden link cost	5000	✓	Penalty cost for links in forbidden sectors (used by Dijkstra’s algorithm, see beginning of Chapter 5).
SA update interval	uniform(3, 5)	✓	Continuous uniform distribution for time between consecutive SA update messages to peers (in seconds).

<sup>1</sup>This is emulation provided by InterceptApp.

## 6.5 Simulation results

As discussed previously, it is important that no packets are leaked to hostile aircraft. If traditional omnidirectional antennas are used, there is a very high risk that a packet is leaked. This risk is reduced if directional antennas are used. However, even when using directional antennas, there is still a risk that a packet is leaked if there are adversary aircraft close to the sender or the receiver (see Figure 5.1). The main benefit of the HDARP protocol is that it considers forbidden sectors so that the risk for leaked packets is substantially reduced.

Tables 6.2 and 6.3 show the reduction of leaked packets when using directional antennas instead of omnidirectional antennas for the five protocols, which the HDARP protocol is compared to for scenarios 1 (R4B4) and 2 (BVR). The table shows that using directional antennas reduced the number of leaked packets with a factor 133 to 222 (depending on the protocol) for Scenario 1 and with a factor of 110 to 7464 for Scenario 2. This means that the reduction of leaked messages due to using directional antennas is very high. However, some packets are still leaked to an adversary aircraft.

Table 6.2: Reduction of the number of leaked packets when going from omnidirectional antennas to directional antennas for each of the studied protocols for Scenario 1 (R4B4).

	<b>AODV</b>	<b>BATMAN</b>	<b>DSDV</b>	<b>DSR-UU</b>	<b>OLSR</b>
Omnidirectional antennas	199,562	211,454	149,051	137,781	147,410
Directional antennas	1256	1588	782	620	762
Reduction ratio	159	133	191	222	194

Figure 6.2 shows the number of packets that are leaked when using directional antennas. The averages and the 99% confidence intervals are shown in the figure. The confidence intervals are very small with the exception of DSR-UU that has a somewhat larger confidence interval than the other protocols. DSR-UU is a complete protocol implementation for the Linux operating system that was later integrated with OMNEST,

Table 6.3: Reduction of the number of leaked packets when going from omnidirectional antennas to directional antennas for each of the studied protocols for Scenario 2 (BVR).

	<b>AODV</b>	<b>BATMAN</b>	<b>DSDV</b>	<b>DSR-UU</b>	<b>OLSR</b>
Omnidirectional antennas	3,138,553	2,524,658	1,393,752	1,311,349	1,194,179
Directional antennas	1186	955	272	11,953	160
Reduction ratio	2646	2644	5143	110	7464



unlike the other protocols, which are pure simulation implementations. However, it is difficult to assess whether this is the reason for the large confidence intervals observed without an in-depth code review, which is outside the scope of this study. The figure shows that the HDARP protocol has (virtually) no leaked packets, whereas the other protocols have a substantial number of leaked packets for the scenarios considered here.

In order not to leak packets, the HDARP protocol sometimes avoids sending packets directly from the sender to the destination, since such direct transmissions could be detected by adversary aircraft (see Figures 4.3 and 5.1). This means that one would expect that the number of hops and, as a consequence of this, the average end-to-end packet delivery time of HDARP could increase compared to protocols that do not consider forbidden sectors. Packet delivery time includes queuing time in each node on the path, as well as transmission and propagation delay for each link of the path.

Figure 6.3 shows that average packet lifetime of the HDARP protocol is longer than the average packet lifetime for four of the other protocols. The difference is small for Scenario 1, but rather significant for Scenario 2. In practice, the type of traffic routed by HDARP will consist mostly of voice-over-IP communication. Conventional wisdom indicates that for this type of traffic, the one-way latency should not exceed 150 ms [37], [38]. This is almost two times the amount of packet life time observed in Scenario 2 and thus does not adversely impact the quality of the voice communication. The average packet lifetime for the AODV protocol is not shown in the figure. The reason for this is that the average packet lifetime of AODV is more than 100 times longer than that of HDARP for Scenario 1 and more than 5 times longer than that of HDARP for Scenario 2.

One drawback of using directional antennas is that a receiver may suffer from destructive interference from two or more simultaneous senders without the senders being aware of the problem (c.f., discussion about unit disk radio in the beginning of this chapter). An example would be if A and B simultaneously sent to C in Figure 4.3 on the same frequency. Therefore, one could expect that the HDARP protocol could suffer from a low packet delivery ratio. Figure 6.4 shows that the packet delivery ratio of the HDARP protocol is on a par with the best of the other protocols for Scenario 1 but a bit lower for Scenario 2. This means that the extra packet loss due to avoiding leakage seems limited. In some situations, HDARP will not be able to find a route that is free from leakage risks. However, in such cases, the packet will still be delivered (see how *weight* is handled in Algorithm 4). This means that the lower packet delivery rate for Scenario 2 is not caused by HDARP not being able to find a route that is free from leakage risks. The very low number of leaked packets for HDARP (see Figure 6.2) shows that HDARP was indeed able to find leakage-free routes in (virtually) all cases. The type of destructive interference mentioned here can be handled in the future by smart antenna arrays that multiplex multiple signals over time, frequency and angle of arrival.

In MANETs, there are two types of packets: packets containing user information (the payload provided through UdpBasicApp), e.g., voice communication between pilots and packets containing control information about the network and the network topology (i.e., routing messages). For each of our two scenarios, the number of packets containing user information is the same for all communication protocols. The number of packets

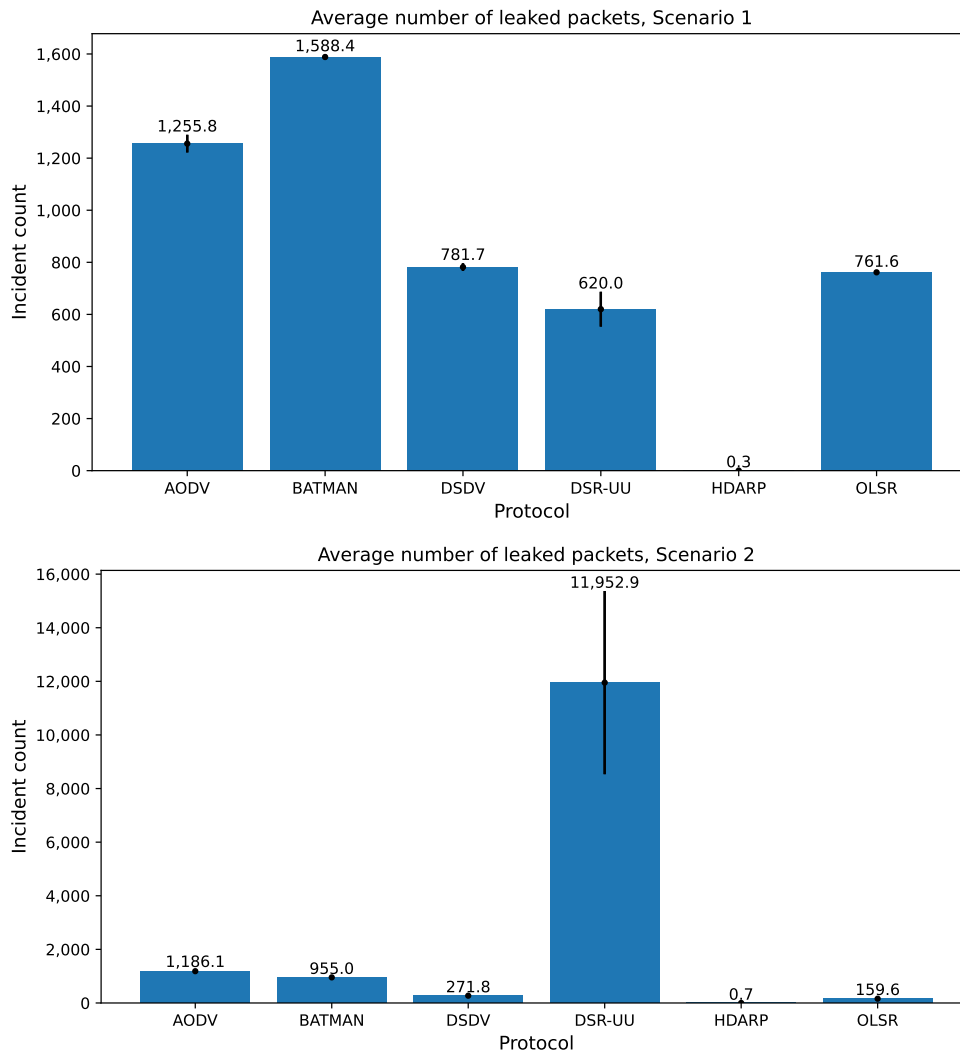


Figure 6.2: Average number of leaked packets when using directional antennas (99% confidence interval), for Scenario 1 (**upper**) and Scenario 2 (**lower**).

containing control information, however, differs between different protocols. Figure 6.5 shows the total number of packets sent for the protocols considered here. The figure shows that DSR-UU and OLSR send a smaller number of packets than the HDARP protocol and that DSDV sends almost the same amount of packets for our two scenarios. This means that for HDARP, the number of packets containing control information is relatively small compared to most of the other protocols.

For HDARP, the control information consists of SA data, and SA data are something that the pilots need for tactical reasons regardless of which communication protocol is used. This means that the control information needed for the HDARP protocol needs to be distributed between the aircraft anyways. As a consequence, Figure 6.5 does not give a completely fair picture of the number of packets sent, since the values for the other protocols do not include communication of SA data. In Table 6.1, we see that

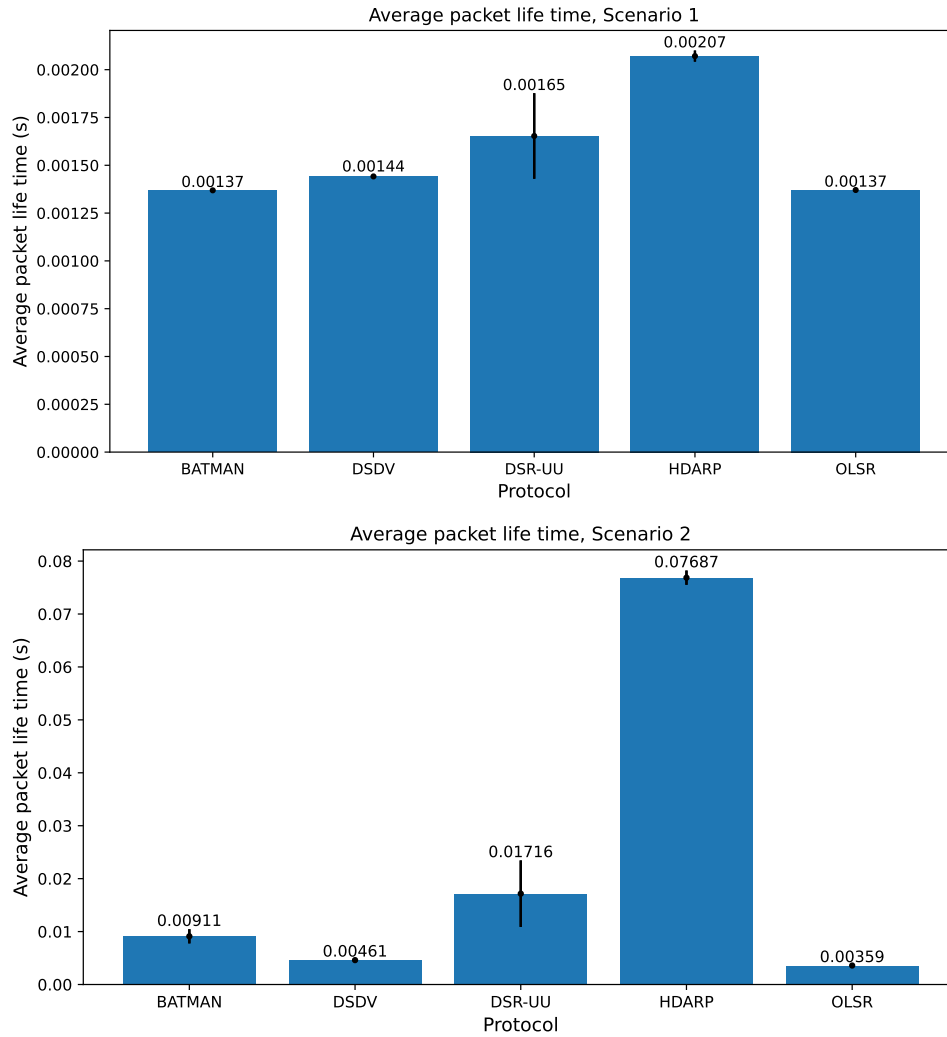


Figure 6.3: Average packet life time in seconds (99% confidence interval) when using omnidirectional antennas for all protocols except HDARP (HDARP uses directional antennas) for Scenario 1 (**upper**) and Scenario 2 (**lower**).

the average time between UDP datagram transmissions is 150 milliseconds (uniform(0.1, 0.2)) and that the average time between SA update messages is 4 s (uniform(3, 5)). This means that during a 12 s interval, we receive 80 UDP datagram transmissions and 3 SA transmissions for each friendly node. Since  $3/80 = 3.75\%$ , one would think that we should multiply the number of sent packets with 1.0375 for all protocols except HDARP. However, SA data are only sent to nodes that are within a one-hop distance from the sender, and due to forbidden sectors, it may not be possible to reach all nodes in one hop. This means that the average number of SA packets sent from each friendly node is somewhat smaller than three during a 12 s interval. If we take this aspect into consideration, all values in Figure 6.5 should be multiplied with a factor of 1.03 (and not 1.0375), except the values for the HDARP protocol. If we consider this multiplication,

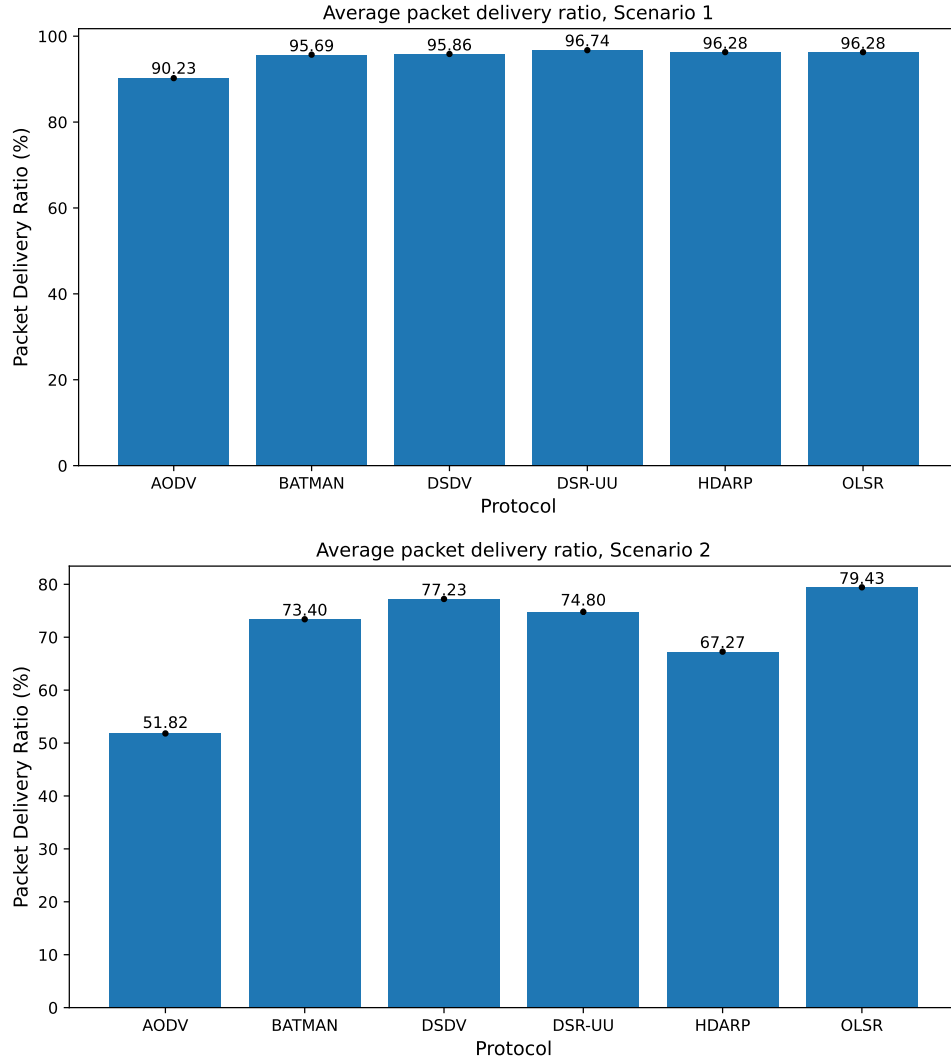


Figure 6.4: Average packet delivery ratio in percent (99% confidence interval) when using omnidirectional antennas for all protocols except HDARP (HDARP uses directional antennas) for Scenario 1 (**upper**) and Scenario 2 (**lower**).

the HDARP protocol will have the second smallest number of packets sent for the R4B4 scenario (DSR-UU will still have the smallest number of sent packets) and the third smallest for the BVR scenario (DSR-UU and OLSR will still have a smaller number of sent packets). Since the SA data are the control information about the network topology for the HDARP protocol, it may seem surprising that some protocols have a lower number of sent packets. The reason for this is that the forbidden sectors in HDARP cause more hops and each extra hop generates a sent packet.

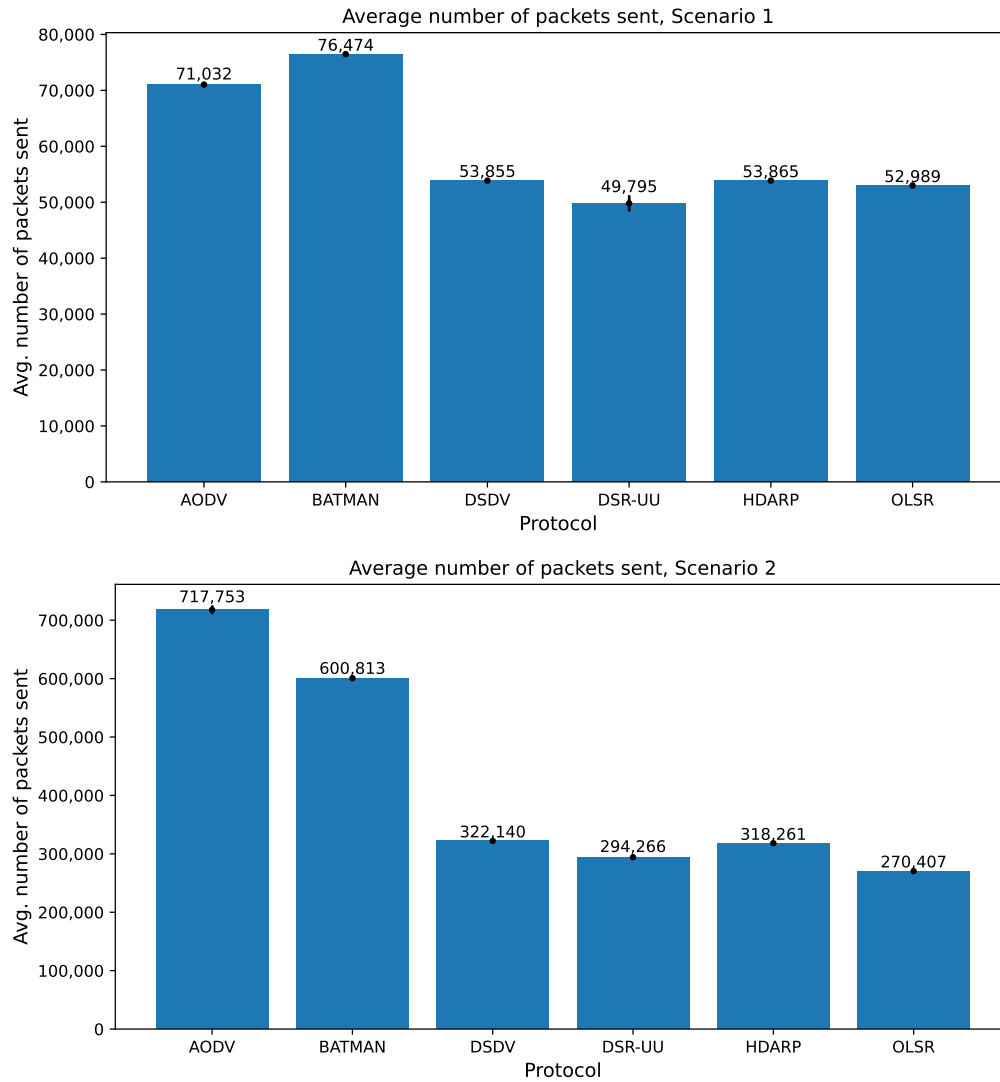


Figure 6.5: Average number of packets sent over the radio interface (99% confidence interval) when using omnidirectional antennas for all protocols except HDARP (HDARP uses directional antennas) for Scenario 1 (**upper**) and Scenario 2 (**lower**).

## 6.6 Analysis and Discussion

Our experiments show that the HDARP protocol avoids adversary detection by minimizing the amount of leaked packets. The HDARP protocol uses situation awareness (SA) data when making routing decisions. The pilots of fighter jets need SA data for completing their missions. This means that SA data are used for two purposes: providing the pilots with mission critical information and for routing communication packets so that they cannot be detected by an adversary.

The HDARP protocol prevents leaking packets to an adversary by proactively trying to avoid transmitting in forbidden sectors. A consequence of this strategy is that a packet

sometimes cannot be sent along a direct line between the sender and the destination. In such cases, the packet needs to be sent via an intermediate node (see Figure 4.3). As a result of this, the number of hops will increase in some cases, and as a consequence, the average packet life time will also increase when we avoid leaking packets. Our experiments quantify this effect for the two scenarios considered. It turns out that compared to most protocols that do not avoid leaked packets, the average packet life time increased significantly for the more complex of the two scenarios (the BVR scenario). However, experts in the area of fighter jet design consider packet leakage to be a major tactical disadvantage from an operational perspective, and the cost in terms of longer average packet life time is therefore regarded as acceptable, depending on scenario at hand.

Our experiments show that using directional instead of omnidirectional antennas will reduce the number of leaked packets by several orders of magnitude. Similar reductions of the detection probability when using directional instead of omnidirectional antennas have been observed by other researchers [39]. The HDARP protocol only works for directional antennas. However, when using directional antennas, simultaneous senders using the same frequency will not detect that the receiver suffers from destructive interference. As a consequence of this, some packets will be lost, resulting in a somewhat lower packet delivery rate for HDARP compared to the best of the omnidirectional protocols. Directional antennas can receive two packets on the same frequency simultaneously if the difference in angle of arrival (AOA) between the two senders is big enough. Our simulator does not consider the angle of arrival, which means that there will be destructive interference regardless of the AOA difference between the senders. This means that the packet delivery rates for HDARP shown in Figure 6.4 are pessimistic and that the cost of using directional antennas and avoiding adversary detection in terms of a somewhat decreased packet delivery rate is acceptable.

The total number of sent packets is relatively small for the HDARP protocol. In fact, it is almost at the same level as the protocol with the smallest number of sent packets (DSR-UU). This means that SA data are a relatively efficient way of representing topology information about the mobile ad hoc network. As discussed previously, the pilots need SA data for completing their mission in any case. If we compensate for this, the difference between the number of packets sent by the HDARP protocol and the number of packets sent by DSR-UU becomes even more marginal. This means that the cost of avoiding adversary detection in terms of an increase in the number of sent packets is minimal and clearly acceptable.

In this paper, we base our evaluation on data from realistic flight scenarios used by the aerospace industry. Unfortunately, many studies of mobile ad hoc networks use very simplistic and unrealistic workload models, e.g., nodes with random movement patterns in a rectangular area [40]. This project was conducted in close cooperation between researchers from academia and aerospace industry experts, which facilitates a high level of realism in the evaluation. In addition, the HDARP protocol is protected by a patent application, which demonstrates the expected importance and practical applicability of the HDARP protocol.

# CHAPTER 7

## Related work

---

Currently, the convergence of several state-of-the-art technologies to create new system-of-system via digitalization within the electromagnetic domain redefines the capability of future airborne communication systems via increased levels of parallelization. Combined with high directivity antennas, novel systems now have the potential to satisfy modern operational requirements for robust networked communication with capabilities such as LPI/LPD, high data rate, security and low latency.

Nonetheless, knowledge is still needed on how a targeted MANET performs in an operational context with different collaborative systems, in expected threat environments and with relevant data traffic requirements, as well as what prerequisites the solution imposes on employed multifunctional antenna systems.

Overall, it is expected that such networks will find applicability in interoperable contexts between multiple platforms throughout different domains. In that respect, the defense industry needs to rapidly develop its familiarity with directed networks, especially for drones and tactical unmanned aerial vehicles (UAVs) for flexible, cost-adapted solutions.

The background for this is that an increasing proportion of aerospace hardware is expected to consist of cooperative platforms, particularly between autonomous systems, thus enabling technologies for this transformation is vital from a future proofing perspective.

### 7.1 Reducing transmission detection

Sharma and Kumar [41] have written a survey of flying ad hoc networks (FANETs) for UAVs. The authors conclude that such networks can be categorized into different types. One important type of network is self-organizing networks, which is what we consider in this paper. One important research area is medium access control (MAC) protocols for FANETs [42]. The MAC protocols for FANETs are challenging for many reasons, e.g., the high speeds of the aircraft create a highly dynamic topology. Some FANETs use directional antennas. Networks with directional antennas offer many advantages, including higher communication capacity through non-interfering simultaneous communication in different directions [43]. Another advantage with using directional antennas is that it becomes easier to avoid detection by hostile nodes; HDARP benefits from this advantage. The challenges on the MAC level in networks using directional antennas have been studied by several researchers [44], [45].

In this paper we focus instead on the network layer where the MANET routing protocols are located. Oubbati et.al. [46] have conducted a survey of routing protocols for FANETs. The authors note that at least 60 routing protocols for FANETs have been suggested. However, most of these 60 protocols are designed for UAVs in non-military contexts, and none of the 60 protocols consider leakage of packets to adversary aircraft, which is the main focus in our case.

We consider communication in an airborne tactical network (ATN) [47] where there are hostile aircraft. Previous studies on ATNs have, however, not considered the presence of hostile aircraft and the implications and restrictions that the presence of hostile aircraft have on routing [48]–[50].

Xiaofeng et al. [51] consider ad hoc networks with hostile nodes, which they call detection systems. The authors define a routing algorithm called MinDP (Minimizing Detection Probability). Compared to routing protocols that do not consider hostile nodes, MinDP reduces the detection probability by 74%. This study differs from our study in several aspects: the nodes in the ad hoc network are not mobile, only two-dimensional space is considered (we consider routing in three-dimensional space), only the main lobe of the directional antenna is considered (we also consider sidelobes) and the evaluation is based on simplistic assumptions about a quadratic two-dimensional space with random placements of nodes (we use mobility data from realistic flight scenarios used by the defense industry).

In mobile ad hoc where the nodes can have a high relative speed, geographical routing is sometimes used [52], [53]. Geographical routing is based on the idea that the source sends a message to the geographic location of the destination. Geographical routing uses the position, speed and (sometimes) acceleration of the nodes in the ad hoc network. Three common approaches when the destination node cannot be reached in a single hop are to select the next node as the node that is closest to the destination node, as the node that the nearest node that makes forward progress, or as the node that is closest to a straight line from the sender to the destination [54], [55]. HDARP is a geographical routing protocol in the sense that the routing decisions are based on the location, speed and acceleration of friendly and adversary nodes. However, the routing decisions are based on an adaptation of Dijkstra’s shortest-path algorithm (see Chapter 5).

## 7.2 Architecture, Design

In this section we summarize work related to the basic principles of general mobile ad hoc networks (MANET) and aeronautical and tactical military networks.

Conti and Giordano [56] review the basic principles of ad hoc mobile networks and discuss research in the field. They conclude that the majority of research related to MANET assumes that such networks will be used for large-scale general consumer applications. The authors conclude that this assumption is unrealistic, and that more specialized applications such as military/battlefield applications are more realistic for MANET. In fact, the authors conclude that the research related MANET lacks real-



ism in several aspects. For instance, the performance evaluations assume unrealistic use cases where mobile nodes move in random patterns in a limited area. It is also noted that most of the research is theoretical and that, implementation, integration and experimentation is missing in most MANET research projects. Most of the results are based on simulations that often lacks credibility, thus compromising the usefulness of the obtained results.

In mobile ad hoc networks where the nodes can have a high relative speed, geographical routing is sometimes used [52], [53]. Geographical routing is based on the idea that the source sends a message to the geographic location of the destination. Geographical routing uses the position, speed and (sometimes) acceleration of the nodes in the ad hoc network. Three common approaches when the destination node cannot be reached in a single hop are to select the next node as the node that is closest to the destination node, as the node that the nearest node that makes forward progress, or as the node that is closest to a straight line from the sender to the destination [54], [55].

Wang et al [57] consider tactical communication systems for military applications. These complex systems combine terrestrial (including ships), airborne, and space-based platforms. These systems are typically mobile and communicate through wireless networks. The authors identify two architectural challenges related to the dynamically changing nature of such networks: (i) the quality of the links (connections) between the nodes changes dynamically, and (ii) the topology of the network also changes dynamically when the nodes move around.

In this report we consider communication in an airborne tactical network [58] where there are hostile aircraft. Previous studies related to airborne tactical networks have, however, not considered the presence of hostile aircraft and the implications and restrictions that the presence of hostile aircraft have on routing [48]–[50].

## 7.3 Specifications, on-track, or well-known

In this section we summarize work related to the basic routing principles of mobile ad hoc networks (MANET) and some important routing protocols.

In 1994 Perkins and Bhagwat [25] did some seminal work when they came up with the idea that each node in the mobile network should act as a specialized router. The authors investigated some modifications of the well-known Bellman-Ford distance-vector routing algorithm. One conclusion from that study was that mobile nodes (computers) modeled as routers can effectively cooperate to build ad hoc networks.

Based on the seminal work from 1994 a number of protocols were defined. In 2003 Perkins et al. [23] defined the ad hoc on-demand distance vector (AODV) algorithm that enables dynamic, self-starting, multihop routing between participating mobile nodes in an ad hoc network. A second version of the AODV protocol was developed by Perkins et al. in 2019 [30]. In 2004 Ogier et al. [59] developed a protocol called TBRPF (Topology Dissemination Based on Reverse-Path Forwarding), that provides hop-by-hop routing along shortest paths to each destination in mobile ad hoc networks. In 2007 Johns-

son et al. [26] defined the dynamic source routing (DSR) protocol, which is a simple and efficient routing protocol designed specifically for use in multi-hop wireless ad hoc networks of mobile nodes. In 2009 Ogier et al. [60] suggested a MANET Extension of the OSPF (Open Shortest Path First) routing protocol using connected dominating Set (CDS) flooding. In 2014 Clausen et al. [27] defined a new version of the OLSR (Optimized Link State Routing) protocol for mobile ad hoc networks. The objectives of this protocol are for each router to: (i) identify all destinations in the network, (ii) identify a sufficient subset of links in the network, in order that shortest routes can be calculated to all available destinations, and (iii) provide a routing set containing these shortest routes from the router to all destinations.

## 7.4 Surveys

In this section we summarize some of the surveys that have been written in the area. We cover both general surveys as well as some surveys on more specific topics that are relevant in our context.

Bekmezci et al. [61] present a general survey of flying ad-hoc networks (FANETs), with a focus on FANETs in multi-UAV (unmanned aerial vehicle) systems. First, they highlight the differences between FANETs, mobile ad-hoc networks (MANETs), and vehicle ad-hoc networks (VANETs). FANETs distinguish themselves from MANETs and VANETs in the following aspects:

- FANET nodes have a much higher mobility degree and a different mobility model, i.e., they fly at high speeds in the sky while MANET and VANET nodes are typically walking / moving persons and cars, respectively.
- The network topology of FANETs changes more frequently than for MANETs and VANETs, mainly due to the higher mobility degree. Further, failure of an UAV or a link failure also affect the topology and often require a topology update.
- Typical distances between FANET nodes are much longer than in MANETs and VANETs, i.e., the communication range in FANETs must be longer, which affects, e.g., the radio links, hardware circuits, and physical layer behavior. A related aspect that affect the radio propagation model is that FANETs generally communicate in the sky where there often is a line-of-sight between the nodes, while MANETs and VANETs communicate close to the ground with no line-of-sight.

Based on the identified characteristics of FANETs as compared to other ad-hoc networks, Bekmezci et al. [61] discussed the most important FANET design considerations. The following FANET design considerations are discussed:

- **Adaptability.** A FANET needs to be highly adaptable for many reasons, e.g., FANET nodes are highly mobile, move fast, and change their location frequently so the nodes distances vary constantly. Further, technical problems such as link

failures and UAV operational failures, as well as environmental conditions affect the topology and routing in FANETs.

- **Scalability.** A FANET needs to ability to handle a large number of nodes, as well as handling nodes both entering and leaving the FANET.
- **Latency.** Latency is an important design aspect for all networks, and especially for FANETs. However, the exact latency requirements are application dependent, and can differ from low-latency real-time requirements to quite long latencies. The authors note that new FANET protocols and algorithms are necessary to develop for delay sensitive multi-UAV applications.
- **UAV platform constraints.** Since the FANET hardware needs to be airborne, the UAV platform may impose constraints on, e.g., weight, power consumption, and space / volume.
- **Bandwidth requirements.** The bandwidth capacity is important, and there are many constraints for its use, e.g., the capacity of the channel, the speed of the UAV, errors on the links, etc. Further, the bandwidth is often shared among several different applications.

Finally, Bekmezci et al. discuss and point out open research issues at (i) the physical layer, e.g., the radio propagation model and the antenna structure, (ii) the MAC layer, e.g., overcoming link quality variations and long distances, (iii) the network layer, e.g., novel routing solutions, (iv) the transport layer, e.g., on reliability, congestion control, and flow control, and finally (v) on cross-layer architectures.

Bujari et al. [62] presents an overview of flying ad-hoc network (FANET) application scenarios and mobility models, with an emphasis on unmanned aerial vehicles (UAVs). Many of the listed FANET application scenarios are based on multi-UAV systems, where several UAVs together solve a task. Examples of application scenarios for multi-UAVs are search and rescue operations, forest fire detection, traffic and urban monitoring, and various applications involving environmental sensing.

Concerning mobility models for FANETs, Bujari et al. divide them into five classes: pure randomized mobility models, time-dependent mobility models, path-planned mobility models, group mobility models, and topology-control-based mobility models. Some of them are purely stochastic, such as the pure randomized and time-dependent models, others semi-random (often a combination of a pre-defined path and some stochastic movements), such as the path-planned and group model, and finally some of the reviewed topology-control-based models contain no stochastic elements. An observation to done is that very few of the mobility models have some connectivity awareness, which is essential in many application scenarios. Finally, Bujari et al. list 12 network simulators along with the different mobility models they implement and support.

Oubbati et al. [63] have done a survey on flying ad-hoc networks (FANETs). Their focus is on FANETs for unmanned aerial vehicles (UAVs). They start by concluding that although FANETs are similar to general mobile ad-hoc networks (MANETs), they

have their own characteristics. For example, groups UAVs are often mission-based which impact the FANET design and their mobility models are often dictated by the mission characteristics and purpose. Further, the highly dynamic topology and flying constraints of FANETs also complicates the routing protocol design. In general, position-based routing demonstrates a high efficiency and resilience to handle the mobility of FANET nodes as compared to topology-based routing. In a succeeding survey [46], Oubbati et al. focus on the routing in FANETs. Also in this survey, they have a focus on FANETs for UAVs. The survey covers the architecture, the constraints, the mobility models, the routing techniques, and the simulation tools dedicated to FANETs.

Quy et al. [64] have published a survey of recent routing metrics protocols used in MANETs. Their survey covers protocol proposals published 2010-2017. Metrics covered in the study are: traffic-based metrics such as delays and packet loss ratio; radio information such as signal strength and signal-to-noise ratio; mobility and location metrics; and energy aspects.

## CHAPTER 8

# Conclusion and Future Work

---

We have defined the Hostile-Direction Aware Routing Protocol (HDARP) that avoids detection by adversary aircraft in airborne tactical networks. HDARP uses directional antennas and avoids adversary detection by using so-called situation awareness (SA) data to determine a route such that the packets are not detected by hostile aircraft. SA data are needed in order for the pilots to perform their mission.

One of the advantages of HDARP, besides avoiding adversary detection, is that it uses already existing SA data for network topology control and routing decisions as well. Based on evaluations using realistic directional antenna models and flight scenarios from the defense industry, we have shown that the major tactical advantage of avoiding adversary detection comes at a relatively small, and clearly acceptable, cost in terms of somewhat longer packet lifetime and marginally lower packet delivery rate. Our evaluations also show that SA data provide a highly efficient way of representing network topology control, and the number of sent packets using HDARP is on a par with the best routing algorithms that do not avoid adversary detection. This means that the cost of avoiding adversary detection in terms of a slight increase of the number of sent packets is negligible.

In general, in this paper, we focus on the algorithmic properties of the protocol and not on the radio transmission protocol. In future work, we will consider looking at the effects of the radio protocol as well: examples include path loss, fading, and shadowing aspects. Further, we might also consider additional flight scenarios, different relations between flight speed and message propagation latencies. Finally, we have not tracked the beam width in our simulations. Theoretically, a narrow beam width decreases the probability of detection but potentially increases the average path length. Conversely, a wide beam width enables direct communication with more nodes, i.e., multicast, but potentially increases the probability of detection. We think that the trade-off between these two is a very interesting aspect that we consider for future work.



# Bibliography

---

- [1] S. R. Saunders and A. Aragón-Zavala, *Antennas and Propagation for Wireless Communication Systems*, 2nd. Wiley, 2007, ISBN: 978-0-470-84879-1.
- [2] B.-N. Cheng, R. Charland, P. Christensen, L. Veytser, and J. Wheeler, “Evaluation of a multihop airborne IP backbone with heterogeneous radio technologies,” *IEEE Transactions on Mobile Computing*, vol. 13, no. 2, Feb. 2014. DOI: 10.1109/TMC.2012.250.
- [3] D. Ilie, H. Grahn, L. Lundberg, A. Westerhagen, B. Granbom, and A. Höök, “Avoiding detection by hostile nodes in airborne tactical networks,” *Future Internet*, vol. 15, no. 6, p. 204, May 2023, ISSN: 1999-5903. DOI: 10.3390/fi15060204. [Online]. Available: <http://dx.doi.org/10.3390/fi15060204>.
- [4] R. Braden, *RFC 1122: Requirements for internet hosts – communication layers*, IETF, Oct. 1989. [Online]. Available: <https://tools.ietf.org/html/rfc1122>.
- [5] K. R. Fall and W. R. Stevens, *TCP/IP Illustrated: The Protocols*, 2nd. Boston, MA, USA: Addison Wesley, 2012, ISBN: 978-0-321-33631-6, ISBN: 978-0-321-33631-6.
- [6] J. L. Burbank, P. F. Chimento, B. K. Haberman, and K. W. T., “Key challenges of military tactical networking and the elusive promise of MANET technology,” *IEEE Communications Magazine*, vol. 44, no. 11, pp. 39–45, Nov. 2006. DOI: 10.1109/COM-M.2006.248156.
- [7] B. Cain, S. Deering, B. Fenner, I. Kouvelas, and A. Thyagarajan, *RFC 3376: Internet group management protocol, version 3*, IETF, Oct. 2002. [Online]. Available: <https://tools.ietf.org/html/rfc3376>.
- [8] J. Schiller, *Mobile Communications*, 2nd. Boston, MA, USA: Addison Wesley, 2003, ISBN: 0-321-12381-6.
- [9] D. Medhi and K. Ramasamy, *Networking Routing: Algorithms, Protocols and Architectures*, 2nd. Morgan-Kaufmann, 2018, ISBN: 978-0-12-800737-2.
- [10] D. Ilie and A. Popescu, “Unicast QoS routing in overlay networks,” in *Next Generation Internet: Performance Evaluation and Applications*, ser. Lecture Notes in Computer Science (LNCS ), D. D. Kouvatsos, Ed., vol. LNCS 5233, ISBN: 978-3-642-02741-3, Berlin Heidelberg, Germany: Springer-Verlag, 2011, pp. 1017–1038. DOI: 10.1007/978-3-642-02742-0.

- [11] A. V. McCree and T. P. Barnweell, "A mixed excitation LPC vocoder model for low bit rate speech coding," *IEEE Transactions on Speech and Audio Processing*, vol. 3, no. 4, pp. 242–250, 1995. DOI: 10.1109/89.397089.
- [12] H. Schulzrinne, S. L. Casner, R. Frederick, and V. Jacobson, *RFC 3550 RTP: A transport protocol for real-time applications*, <https://www.rfc-editor.org/rfc/rfc3550>. Last visited: 2023-04-11., IETF, Jul. 2003. [Online]. Available: <https://tools.ietf.org/html/rfc3550>.
- [13] *Wideband networking waveform OFDM PHY: Physical layer implementation of WNW on the SDR-4000 platform*, Spectrum Signal Processing, 2009. [Online]. Available: [https://web.archive.org/web/20140312224424/http://www.spectrumsignal.com/products/pdf/wnw\\_ofdm\\_web.pdf](https://web.archive.org/web/20140312224424/http://www.spectrumsignal.com/products/pdf/wnw_ofdm_web.pdf).
- [14] "IEEE standard for Ethernet," *IEEE Std 802.3-2018 (Revision of IEEE Std 802.3-2015)*, pp. 1–5600, 2018. DOI: 10.1109/IEEESTD.2018.8457469.
- [15] E. W. Dijkstra, "A note on two problems in connection with graphs," *Numerische Mathematik*, vol. 1, pp. 269–271, 1959.
- [16] T. H. Cormen, C. E. Leiserson, and R. L. Rivest, *Introduction to Algorithms*, 2nd. Cambridge, MA, USA: The MIT Press, 2001, ISBN: 0-262-53196-8.
- [17] A. Goldsmith, *Wireless Communications*. New York, NY, USA: Cambridge University Press, 2005, 8th printing, ISBN: 978-0-521-83716-3.
- [18] A. Varga and R. Hornig, "An overview of the OMNeT++ simulation environment," in *Simutools*, Marseille, France, Mar. 2008.
- [19] (). "Omnet++." Last visited: 2023-04-07, [Online]. Available: <https://omnetpp.org>.
- [20] (). "Inetmanet." Last visited: 2023-04-07, [Online]. Available: <https://github.com/aarizaq/inetmanet-4.x>.
- [21] (). "Inet." Last visited: 2023-04-07, [Online]. Available: <https://inet.omnetpp.org/>.
- [22] A. Virdis and M. Kirsche, Eds., *Recent Advances in Network Simulation: The OMNeT++ Environment and Its Ecosystem*, ser. EAI/Springer Innovations in Communication and Computing. Cham, Switzerland: Springer Nature Switzerland AG, 2019, ISBN: 978-3-030-12844-9.
- [23] C. E. Perkins, E. M. Belding-Royer, and S. R. Das, *RFC 3561: Ad hoc on-demand distance vector (AODV) routing*, <https://www.rfc-editor.org/rfc/rfc3561>. Last visited: 2023-04-08., IETF, Jul. 2003. [Online]. Available: <https://www.rfc-editor.org/rfc/rfc3561>.
- [24] Open-Mesh.net. (2023). "B.A.T.M.A.N. - (better approach to mobile ad-hoc networking)." Last visited: 2023-04-08., [Online]. Available: <https://www.open-mesh.org/projects/open-mesh/wiki>.



- [25] C. E. Perkins and P. Bhagwat, “Highly-dynamic destination-sequenced distance-vector routing for mobile computers (DSDV),” in *ACM SIGCOMM '94*, London, UK, 1994.
- [26] D. B. Johnson, D. A. Maltz, and Y.-C. Hu, *RFC 4728: The dynamic source routing protocol (DSR) for mobile ad hoc networks for IPv4*, <https://www.rfc-editor.org/rfc/rfc4728>. Last visited: 2023-04-08., IETF, Feb. 2007. [Online]. Available: <https://www.rfc-editor.org/rfc/rfc4728>.
- [27] T. H. Clausen, C. Dearlove, P. Jacquet, and U. Herberg, *RFC 7181: The optimized link state routing protocol version 2 (OLSRv2)*, <https://www.rfc-editor.org/rfc/rfc7181>. Last visited: 2023-04-08., IETF, Apr. 2014. [Online]. Available: <https://tools.ietf.org/html/rfc7181>.
- [28] H. Lundgren, *Implementation and real-world evaluation of routing protocols for wireless ad hoc networks*, Licentiate thesis, Uppsala, Sweden, Nov. 2002.
- [29] C. E. Perkins, S. Ratliff, and J. Dowdell, *Dynamic manet on-demand (AODVv2) routing*, draft-ietf-manet-dymo-26. <https://www.ietf.org/archive/id/draft-ietf-manet-dymo-26.txt>. Last visited: 2023-04-08., IETF, Feb. 2013. [Online]. Available: <https://tools.ietf.org/html/draft-ietf-manet-dymo-26>.
- [30] C. E. Perkins, S. Ratliff, J. Dowdell, L. Steenbrink, and V. Pritchard, *Ad hoc on-demand distance vector version 2 (AODVv2) routing*, draft-perkins-manet-aodvv2-03. <https://www.ietf.org/archive/id/draft-perkins-manet-aodvv2-03.txt>. Last visited: 2023-04-08., IETF, Feb. 2019. [Online]. Available: <https://tools.ietf.org/html/draft-perkins-manet-aodvv2-03.txt>.
- [31] M. Louizi, “Implementierung des Ad-hoc-Routing-Protokolls DYMO,” Bachelor Thesis, Department of Computer Science, Erlangen, Germany, Jun. 2006.
- [32] (). “Netfilter: Firewalling, NAT, and packet mangling for linux.” Last visited: 2023-04-08, [Online]. Available: <https://www.netfilter.org>.
- [33] V. Inzillo, F. De Rango, and A. A. Quintana, “Supporting 5G wireless networks through IEEE802.11ac standard with new massive MIMO antenna system module design in OMNeT++ simulator,” in *8th International Conference on Simulation and Modeling Methodologies, Technologies and Applications (SIMULTECH)*, Porto, Portugal, Jul. 2018.
- [34] D. C. Plummer, *RFC 826: An ethernet address resolution protocol – or – converting network protocol addresses to 48.bit ethernet address for transmission on ethernet hardware*, <https://www.rfc-editor.org/rfc/rfc826.txt>. Last visited: 2023-04-08., 1982. [Online]. Available: <https://www.rfc-editor.org/rfc/rfc826.txt>.
- [35] N. A. T. O. (NATO), *The 600 bit/s, 1200 bit/s and 2400 bit/s NATO interoperable narrow band voice coder*, STANAG No. 4591, 2006.
- [36] M. Matsumoto and T. Nishimura, “Mersenne Twister: A 623-dimensionally equidistributed uniform pseudo-random number generator,” *ACM Transactions on Modeling and Computer Simulation*, vol. 8, no. 1, pp. 3–30, Jan. 1998.

- [37] ITU, *One way transmission time*, ITU-T Recommendation G.114, May 2003.
- [38] A. Markopoulou, F. Tobagi, and M. Karam, “Assessing the quality of voice communications over Internet backbones,” *IEEE/ACM Transactions on Networking*, vol. 11, no. 5, pp. 747–760, Oct. 2003.
- [39] X. Lu, F. D. Wicker, D. Towsley, Z. Xiong, and P. Lio’, “Detection probability estimation of directional antennas and omni-directional antennas,” English, *Wireless personal communications*, vol. 55, no. 1, pp. 51–63, 2010.
- [40] M. Conti and S. Giordano, “Multihop ad hoc networking: The theory,” English, *IEEE Communications Magazine*, vol. 45, no. 4, pp. 78–86, 2007.
- [41] V. Sharma and R. Kumar, “Cooperative frameworks and network models for flying ad hoc networks: A survey,” *Concurrency and Computation: Practice and Experience*, vol. 29, no. 4, e3931, 2017, e3931 cpe.3931. DOI: <https://doi.org/10.1002/cpe.3931>. eprint: <https://onlinelibrary.wiley.com/doi/pdf/10.1002/cpe.3931>. [Online]. Available: <https://onlinelibrary.wiley.com/doi/abs/10.1002/cpe.3931>.
- [42] M. Y. Arafat, S. Poudel, and S. Moh, “Medium access control protocols for flying ad hoc networks: A review,” *IEEE Sensors Journal*, vol. 21, no. 4, pp. 4097–4121, 2021. DOI: 10.1109/JSEN.2020.3034600.
- [43] S. Yi, Y. Pei, and S. Kalyanaraman, “On the capacity improvement of ad hoc wireless networks using directional antennas,” in *Proceedings of the 4th ACM International Symposium on Mobile Ad Hoc Networking and Computing*, ser. Mobi-Hoc ’03, Annapolis, Maryland, USA: Association for Computing Machinery, 2003, pp. 108–116, ISBN: 1581136846. DOI: 10.1145/778415.778429. [Online]. Available: <https://doi.org/10.1145/778415.778429>.
- [44] F. Babich, M. Comisso, A. Crismani, and A. Dorni, “On the design of mac protocols for multi-packet communication in iee 802.11 heterogeneous networks using adaptive antenna arrays,” *IEEE Transactions on Mobile Computing*, vol. 14, no. 11, pp. 2332–2348, 2015. DOI: 10.1109/TMC.2014.2385058.
- [45] G. Wang and Y. Qin, “Mac protocols for wireless mesh networks with multi-beam antennas: A survey,” in *Advances in Information and Communication*, K. Arai and R. Bhatia, Eds., Cham: Springer International Publishing, 2020, pp. 117–142, ISBN: 978-3-030-12388-8.
- [46] O. S. Oubbati, M. Atiquzzaman, P. Lorenz, M. H. Tareque, and M. S. Hossain, “Routing in flying ad hoc networks: Survey, constraints, and future challenge perspectives,” *IEEE Access*, vol. 7, pp. 81 057–81 105, Jun. 2019. DOI: 10.1109/ACCESS.2019.2923840.
- [47] B.-N. Cheng, F. J. Block, B. R. Hamilton, D. Ripplinger, C. Timmerman, L. Veytser, and A. Narula-Tam, “Design considerations for next-generation airborne tactical networks,” *IEEE Communications Magazine*, vol. 52, no. 5, pp. 138–145, 2014. DOI: 10.1109/MCOM.2014.6815904.

- [48] Y. Pan, N. Lyu, and C. Yang, "Gor: Group-oblivious multicast routing in airborne tactical networks under uncertainty," *Journal of Network and Computer Applications*, vol. 207, p. 103 509, 2022, ISSN: 1084-8045. DOI: <https://doi.org/10.1016/j.jnca.2022.103509>. [Online]. Available: <https://www.sciencedirect.com/science/article/pii/S1084804522001503>.
- [49] J. Miao, N. Lv, K. Chen, Q. Gao, and X. Wang, "Dynamic reliability-aware virtual network embedding for airborne tactical networks," English, *Wireless communications and mobile computing*, vol. 2022, 2022.
- [50] K. Chen, S. Zhao, and N. Lv, "Network monitoring information collection in the sdn-enabled airborne tactical network," English, *International journal of aerospace engineering*, vol. 2018, pp. 1–20, 2018.
- [51] X. Lu, D. Towsley, P. Lio', F. Wicker, and Z. Xiong, "Minimizing detection probability routing in ad hoc networks using directional antennas," English, *EURASIP journal on wireless communications and networking*, vol. 2009, no. 1, 2009.
- [52] K. Peters, A. Jabbar, E. K. Cetinkaya, and J. P. G. Sterbenz, "A geographical routing protocol for highly-dynamic aeronautical networks," in *2011 IEEE Wireless Communications and Networking Conference*, 2011, pp. 492–497. DOI: 10.1109/WCNC.2011.5779182.
- [53] A. Swidan, S. Khattab, Y. Abouelseoud, and H. Elkamchouchi, "A secure geographical routing protocol for highly-dynamic aeronautical networks," English, vol. 2015-, IEEE, 2015, pp. 708–713, ISBN: 9781509000739;1509000739;
- [54] C. Lemmon, C. Lui, and I. Lee, "Review of location-aware routing protocols," *AISS*, vol. 2, pp. 132–143, Jun. 2010. DOI: 10.4156/aiss.vol2.issue2.15.
- [55] J. Agrawal and M. Kapoor, "A comparative study on geographic-based routing algorithms for flying ad-hoc networks," English, *Concurrency and computation*, vol. 33, no. 16, n/a, 2021.
- [56] M. Conti and S. Giordano, "Multihop ad hoc networking: The theory," English, *IEEE Communications Magazine*, vol. 45, no. 4, pp. 78–86, 2007.
- [57] M.-C. Wang, Y. S. Chuang, S. A. Davidson, and B. Liu, "In the design of tactical communication systems," in *Proceedings of IEEE SysCon*, Vancouver, BC, Canada, Apr. 2018. DOI: 10.1109/SYSCON.2018.8369512.
- [58] B.-N. Cheng, F. J. Block, B. R. Hamilton, D. Ripplinger, C. Timmerman, L. Veytser, and A. Narula-Tam, "Design considerations for next-generation airborne tactical networks," *IEEE Communications Magazine*, pp. 138–145, May 2014.
- [59] R. G. Ogier, F. L. Templin, and M. G. Lewis, *RFC 3684: Topology dissemination based on reverse-path forwarding (TBRPF)*, IETF, Feb. 2004. [Online]. Available: <https://tools.ietf.org/html/rfc3684>.
- [60] R. G. Ogier and P. Spagnolo, *RFC 5614: Mobile ad hoc network (MANET) extension of OSPF using connected dominating set (CDS) flooding*, IETF, Aug. 2009. [Online]. Available: <https://tools.ietf.org/html/rfc5614>.

- [61] I. Bekmezci, O. K. Sahingoz, and Ş. Temel, “Flying ad-hoc networks (FANETs): A survey,” *Ad Hoc Networks*, vol. 11, pp. 1254–1270, Jan. 2013. DOI: 10.1016/j.adhoc.2012.12.004.
- [62] A. Bujari, C. T. Calafate, J.-C. Cano, P. Manzoni, C. E. Palazzi, and D. Ronzani, “Flying ad-hoc network application scenarios and mobility models,” *International Journal of Distributed Sensor Networks*, vol. 13, no. 10, Sep. 2017. DOI: 10.1177/1550147717738192.
- [63] O. S. Oubbati, A. Lakas, F. Zhou, M. Güneş, and M. B. Yagoubi, “A survey on position-based routing protocols for flying ad hoc networks (FANETs),” *Vehicular Communications*, vol. 10, pp. 29–56, Nov. 2017. DOI: 10.1016/j.vehcom.2017.10.003.
- [64] V. K. Quy, N. T. Ban, V. H. Nam, and D. M. Tuan, “Survey of recent routing metrics and protocols for mobile ad-hoc networks,” *Journal of Communications*, vol. 14, no. 2, pp. 110–120, Feb. 2019. DOI: 10.12720/jcm.14.2.110-120.